



**SCHOOL OF ADVANCED STUDIES OF THE ROMANIAN
ACADEMY**

**DOCTORAL SCHOOL OF CHEMICAL SCIENCES
PETRU PONI INSTITUTE OF MACROMOLECULAR
CHEMISTRY
CHEMISTRY Field**

***NEW SILICON-CONTAINING COMPOUNDS AND
MATERIALS FOR BIOMEDICAL APPLICATIONS***

PhD THESIS SUMMARY

PhD supervisor:
CS I. DR. MARIA CAZACU

PhD student:
Med.Bioing. BIANCA-IULIA CIUBOTARU

2024

Acknowledgements

It is with great respect and deep gratitude that I thank all those who have contributed to the development and completion of this scientific endeavour so important in my training as a researcher.

*I would like to thank the scientific advisor, **Dr. Maria Cazacu**, for the patience, effort and dedication she has always demonstrated in sharing her vast knowledge, the wisdom with which it has been offered attests to her lifelong passion for the field.*

*I would like to express my gratitude for the constant help and encouragement I received throughout my PhD internship to **Dr. Mirela-Fernanda Zaltariov**, thanks to whose enthusiasm it was possible to carry out my work in a solid team, distinguished by competence and involvement. I will always cherish the beginning of our collaboration, opportunity for which I am grateful to **Prof. Vereștiuc**.*

*I am permanently grateful and would like to thank all of my colleagues in "**Laboratory 62**", **Dr. Carmen Racleș**, **Dr. Sergiu Shova**, **Dr. Mihaela Dascălu**, **Dr. Adrian Bele**, **Dr. George Știubianu**, **Dr. Alexandra Bargan**, **Dr. Codrin Țugui**, **Dr. Alina Soroceanu**, **Ing. Roxana Solomon**, **Dr. Alexandru Stoica** and **Dr. Mădălin Dămoc**, for their support, continuous collaboration and for all the beautiful moments spent together.*

*Gratitude to the scientific reviewers, **Prof. Dr. Liliana Vereștiuc**, **Prof. Dr. Geta David** and **Dr. Mariana Pinteală**, for their availability, time and patience in evaluating this thesis.*

Sincere gratitude to my family, especially my parents, for their unwavering and unconditional help, support and encouragement.

I also wish to thank the Romanian Academy and the 5D-nanoP, 2D-PerMONSil and SilArtSkin projects for their financial support during my PhD training.

With great consideration,

Bianca-Iulia Ciubotaru

CONTENTS

LIST OF ABBREVIATIONS AND SYMBOLS	1
INTRODUCTION	6
LITERATURE SURVEY	6
CHAPTER I. CONCEPTUAL AND BIBLIOGRAPHICAL REFERENCES ON SILICONES FOR BIOMEDICAL APPLICATIONS	6
I.1. Silicone compounds and materials	6
I.1.1. Definition of silicones	6
I.1.2. Properties of silicones	6
I.1.3. Special features of silicones of interest for biomaterials	9
I.1.3.1. Key concepts in biomaterials: their definition and relevance	9
I.1.3.2. Interaction of silicone materials with biological systems: advantages and challenges	11
I.1.3.3. Silicon-containing compounds of biomedical interest: current uses	13
I.1.3.3.1. Silicones: oligo-/polysiloxanes, silicone networks/elastomers	15
I.1.3.3.2. Silico-organic compounds	17
I.1.3.3.3. Silica (crystalline, amorphous, mesoporous)	20
I.2. Techniques for synthesis and chemical modification of silicon-based compounds and materials	23
I.2.1. Obtaining oligo-/polysiloxanes	23
I.2.2. Chemical modification of oligo-/polysiloxanes	25
I.2.3. Obtaining of silicone elastomers	27
I.2.4. Physical and chemical modification of silicone materials	30
I.2.5. Silica obtaining	31
I.3. Safety and toxicity of silicones	32
I.3.1. Toxicity of linear silicones	33
I.3.2. Toxicity of cyclic silicones	34
I.3.3. Toxicity of silicone micro/nanoparticles	35
I.4. Biomedical applications of silicone materials	41
I.5. Challenges in the field of biomaterials in general and silicones in particular	43
ORIGINAL CONTRIBUTIONS	49
CHAPTER II - SILATRAN DERIVATIVES	49
II.1. Introduction	44
II.2. 1-(5-nitrosalicyliminopropyl)silatrane derivative (SIL-BS) obtaining	45
II.3. Structural characterisation of the SIL-BS compound	46
II.3.1. FTIR Spectroscopy	46
II.3.2. NMR Spectroscopy	46
II.3.3. UV-Vis Spectroscopy	46
II.3.4. Single-crystal X-ray diffraction	47
II.4. Evaluation of the application potential of silatrans in the biomedical field	49
II.4.1. Hydrolytic stability of SIL-BS derivative in PBS medium mimicking physiological conditions	49
II.4.2. Cell culture study	50
II.4.3. Human serum proteins binding ability evaluation	53

II.4.3.1. UV-vis spectroscopy and fluorescence	54
II.4.3.2. NMR Spectroscopy	57
II.4.3.3. Circular dichroism	57
II.4.3.4. Molecular docking	59
II.4.4. Bio- and mucoadhesion	61
II.4.5. Antimicrobial activity	62
II.5. Conclusions	65
CHAPTER III - MODIFIED MESOPOROUS SILICA	72
III.1. Introduction	67
III.2. Preparation of mesoporous silica particles (MSP)	70
III.2.1. DOX loading in mesoporous silica (samples D1-D5)	72
III.3. Characterisation of DOX-loaded MS systems (D1-D5)	73
III.3.1. FTIR Spectroscopy	73
III.3.2. DLS analysis and Zeta potential	76
III.3.3. MS morphology before and after DOX loading	78
III.4. DOX release studies from silica	80
III. 5. Evaluation of the biomedical application potential of functionalized mesoporous silica	84
III.5.1. Cytotoxicity evaluation of DOX-loaded MS samples	84
III.5.2. Antimicrobial activity	86
III.5.3. Bio- and mucoadhesive evaluation of functionalized mesoporous silica	88
III.6. Conclusions	91
CHAPTER IV. COVALENT SILICONE NETWORKS	97
IV.1. Introduction	92
IV. 2. Materials characterisation	94
IV. 2. 1. Structural analysis	94
IV. 2. 2. Cross-linking density	97
IV. 2. 3. Static contact angle	98
IV. 2. 4. Film surface morphology	99
IV.2.5. Hydrolytic and enzymatic stability	100
IV.3. Evaluation of the application potential of covalent silicone networks in the biomedical field	101
IV.3.1. Determination of biocompatibility by evaluation of surface free energy using the contact angle method	101
IV.3.2. Cell adhesion	105
IV.3.3. Evaluation of antimicrobial activity of covalent silicone networks	106
IV.3.4. Bio- and mucoadhesion	107
IV.4. Conclusions	110
CHAPTER V. SUPRAMOLECULAR SILICONE NETWORKS	116
V.1. Introduction	111
V.2. Obtaining supramolecular networks	113
V.2.1. Obtaining supramolecular silicone networks based on functionalized polysiloxanes (SN1-SN3)	113
V.2.2. Obtaining supramolecular silicone networks based on functionalized polysiloxanes and oligosilsesquioxanes (SN4, SN5)	114
V.3. Characterisation of supramolecular networks	114

V.3.1. Structural characterisation of supramolecular networks	114
V.3.2. Evidence of supramolecular interactions by fluorimetric analysis	117
V.3.3. Thermal behaviour of supramolecular networks	119
V.3.4. Mechanical behaviour of supramolecular networks	122
V.3.5. Study of the dielectric properties of supramolecular networks	124
V.3.6. Self-repairing capacity of supramolecular networks	125
V.3.6.1. Study of the reversibility of supramolecular interactions by FTIR spectroscopy	126
V.3.6.2. Study of the reversibility of supramolecular interactions by dielectric spectroscopy	131
V.4. Evaluation of the biomedical application potential of supramolecular networks	132
V.4.1. Biocompatibility assessment of supramolecular networks	132
V.4.2. Antimicrobial activity of supramolecular networks	133
V.4.3. Evaluation of wetting capacity by static contact angle	135
V.4.3.1. Swelling capacity of supramolecular networks	135
V.4.4. Bio- and mucoadhesion analysis of supramolecular networks	137
V.5. Conclusions	139
CHAPTER VI - DUAL SILICONE COVALENT / SUPRAMOLECULAR POROUS NETWORKS	141
VI.1. Introduction	141
VI.2. Obtaining porous networks	143
VI.3. Characterisation of porous networks	145
VI.3.1. Structural analysis	145
VI.3.2. Reversibility of carbamate bonds	148
VI.3.3. Porous networks morphology	149
VI.3.4. Water vapour sorption capacity	151
VI.3.5. Thermal behaviour of porous networks	152
VI.3.6. Dielectric properties analysis	153
VI.3.7. Mechanical behaviour of porous networks	154
VI.3.8. Relative capacitance modification	156
VI.4. Evaluation of the application potential of porous networks in the biomedical field	159
VI.4.1 <i>In vitro</i> biocompatibility assessment	160
VI.4.2. Antimicrobial activity	162
VI. 4.3. Hydrolytic stability of porous networks	164
VI.5. Conclusions	165
CHAPTER VII - GENERAL CONCLUSIONS	167
PERSPECTIVES	172
SCIENTIFIC ACTIVITY AND DISSEMINATION	173
BIBLIOGRAPHY	179
ANNEX I - MATERIALS AND METHODS	207
ANNEX II - SILATRAN DERIVATIVES	213
ANNEX III - MODIFIED MESOPOROUS SILICA	222
ANNEX IV - COVALENT NETWORKS	224
ANNEX V - SUPRAMOLECULAR NETWORKS	228
ANNEX VI - POROUS NETWORKS	245

INTRODUCTION

Context of the research and importance of the topic

The biomedical field is an interdisciplinary field that involves the application of concepts and techniques from biology, chemistry, physics, engineering and other disciplines for the development of technologies, devices, instruments and materials to diagnose, treat (through medical therapy or regenerative medicine) or monitor the health of individuals. Benefiting from significant advances in the development of advanced materials and innovative technologies, the biomedical field has seen remarkable progress in recent decades. An important place in this category of materials is occupied by silicon-based materials. Silicon, the second most abundant element in the earth's crust, is mainly known for its use in the electronics industry, but the unique properties of silicon-based materials often make them the first choice in the biomedical field as well. The application of silicones as biomaterials dates back to the 1950s as coatings for syringes, in dentistry for impressions [1], and since the early 1960s for breast implants, becoming of great interest for reconstructive plastic surgery [2]. Over time, these materials have also been increasingly sought after for other biomedical applications, such as in dental prosthetics, cytoplasmic engineering, cell growth, contact lenses, joint implants, heart valves, high-sensitivity biosensors, etc [3]. The surface activity of polysiloxanes is one of their most important characteristics from the perspective of their biomedical and engineering applicability [3]. Also, their chemical and thermal stability, hydrophobicity, hemocompatibility and high oxygen permeability make them useful for medical devices intended for transporting body fluids [1,2]. Due to their low inherent toxicity, pure silicones have a low risk of secondary biological reactions, thus enjoying widespread recognition and acceptance in the medical industry [4]. The versatility of silicone chemistry, multiple options for formulating silicone composites and their vulcanization make silicones readily adaptable materials for various biomedical applications. Some silicon derivatives, such as surfactant silicones (dimethicone), administered orally, have been shown to have mucoprotective characteristics with antipruritic and antacid action [5].

Even though the human body ingests silicon compounds daily through drinking water, inhaled air (as silicon-containing dust) and about 0.5 g from food, especially plant foods, silicon does not seem to accumulate in the body (its content in the human body does not exceed a few grams) and does not seem to have any effects on the body. All these aspects have led to the idea that silicon is inert and unnecessary [6]. Generally, biochemical processes involving silicon are poorly understood although, according to studies reported to date, it may play a role in biological activity. While C-C or

C-H bonds are formed in living processes, Si or Si-C analogues have not been detected and are only obtained in the laboratory. Thus, identifying the response of living organisms to the administration of synthetic compounds containing such bonds is challenging [7]. Silicon-based derivatives are used as excipients in topical and transdermal medicinal products, topically applied skin creams and ointments [3-5]. Silicone polymers may also be suitable candidates for steroid delivery in hormone replacement therapies [8,9]. Another category of silicon-based materials is mesoporous silica. It has a high capacity for drug loading and provides controlled release of bioactive compounds compared to amorphous colloidal silica if properly functionalized [10].

The aim of the thesis

Taking into account the existing challenges to develop new drugs and biomaterials as efficient as possible to cover a wide range of requirements, as well as the experience in the field of silicones of the team in which the author - a PhD student with bachelor's and master's degrees in medical bioengineering - works, it seemed logical to choose a research topic that would benefit from this context and contribute to the development of the field. As a result, this thesis aims to approach a theme that uses silicone derivatives as derivatization platforms for the development of compounds, materials and devices of biomedical interest. These compounds and materials can be active medicinal principles, controlled drug delivery systems, for tissue regeneration or can be used in sensory sensing.

The properties, including those of bioapplicative interest, as well as the safety of use of polysiloxanes, differ according to structure, molecular weight, polydispersity, attached chemical groups, etc [11]. Therefore, controlled synthesis and detailed knowledge of the structural characteristics of these compounds are absolutely necessary to identify their bioapplicative potential. Silicones are platforms available for chemical modification to produce compounds with special properties. By attaching different pharmaceutical moieties to the same substrate, a wide range of biologically active compounds can be obtained. At each silicon atom there is at least one organic radical which may or may not be functionalised, so that the density of functional groups on the chain can be varied within very wide limits depending on requirements and needs. Taking into account the versatility of silicones and the wide possibilities of diversification, either by reactions specific to silicone chemistry or by reactions known from organic chemistry, this thesis proposes original research directions on the use of siloxanes or silanes by addressing two routes: the development of silicone compounds and matrices with morphology suitable for drug loading or being themselves biologically

active or reactive, and the design of linear oligodimethylsiloxanes of different sizes and architectures ("end- or chain-functionalized"), capable of binding through chemical bonds or self-assembling through physical interactions. In this context, the thesis aims to develop new silicon-based compounds and materials, to characterize them from a structural point of view, their properties and their medical application potential, and to make significant contributions to the current scientific and medical field.

Thesis objectives

- Obtaining and studying silicone derivatives with biological/medicinal activity from the silatran category.

- Development of reproducible methods for the synthesis of mesoporous silica particles modified with different functional and/or organic groups and testing their suitability and efficiency for the transport and delivery of an active anticancer therapeutic agent - doxorubicin.

- Evaluation of covalently cross-linked silicone films by different chemical approaches (condensation, hydrosilylation, thiol-ene addition, peroxide) in view of their use as biomaterials.

- Obtaining supramolecular, dynamic silicone networks based on (linear or polyhedral) pendant functionalized polysiloxanes with groups capable of forming hydrogen bonds and evaluating their reversibility and self-healing capacity, behavior in biological environments and application potential.

- Study of processes to obtain dual (covalent/supramolecular cross-linked) porous silicone networks, characterization, evaluation of their biocompatibility and suitability for capacitive pressure sensors.

A thorough understanding of the potential of these compounds and materials will enable new and effective solutions to address current health problems.

Thesis structure

The PhD thesis "New silicon-containing compounds and materials for biomedical applications" contains six chapters, structured in two parts, as follows: **PART I** contains **CHAPTER I** dedicated to the literature review on the aspects of interest for the research developed in the thesis: theoretical notions about the physicochemical properties of silicones, characteristics that recommend them as biomaterials and ways to use them in medicine and bioengineering, as well as notions about the safety and toxicity of silicones in different forms (linear, cyclic, nano- or microparticles, films) and their applications. This chapter also includes introductory notions and literature data on silatrans,

functionalized mesoporous silica particles, covalent, supramolecular and porous silicone networks, which are the objects of study of the thesis.

The second part contains the original contributions of the thesis and is structured in five chapters including the derivation, characterization and evaluation of the bioapplicative potential of the newly developed silicon-containing compounds and materials as follows:

CHAPTER II covers the obtaining and characterisation of an organic-anorganic structure by chemical attachment of 5-nitrosalicylaldehyde to 1-(3-aminopropyl)silatrane, including the methods of obtaining and structurally characterising it by IR, NMR and UV-Vis spectroscopy, as well as single crystal X-ray diffraction. Experimental determinations of hydrolytic stability, protein binding capacity, mucoadhesion, antitumor and antimicrobial activity highlight the potential use of these compounds as antitumor agents.

CHAPTER III addresses the topic of mucoadhesive and bioactive mesoporous silica particles as doxorubicin (DOX) carriers for cancer therapy and includes the preparation method of surface-modified silica with organic (methyl) and/or functional (amino and hydroxyl) groups, characterization of the prepared DOX-loaded particles by: FTIR, DLS and Zeta potential spectroscopy, morphological analysis, release studies of the active therapeutic agent. To determine the applicative potential, cytotoxicity studies were performed, antimicrobial activity was analysed and bio- and mucoadhesion of the particles were evaluated.

CHAPTER IV includes the study of covalent silicone networks, characterized in terms of structure, cross-link density, contact angle and surface morphology of the materials, estimating biocompatibility by calculating surface free energy, cell adhesion and evaluating antimicrobial activity and bio-/mucoadhesion to determine properties of biological interest.

CHAPTER V covers the obtaining of supramolecular networks using different types of functionalized polysiloxanes, and the structural, thermal, mechanical, dielectric and wettability characterization of the obtained materials, as well as the study of the self-repairing capacity of supramolecular networks, both by actual demonstrations and by IR and dielectric spectroscopy. The application potential of these materials was assessed by evaluating biocompatibility, antimicrobial activity, swelling capacity in different media, and bio- and mucoadhesion on different mucous membranes of the gastrointestinal tract.

CHAPTER VI describes the obtaining of porous networks and their characterization by structural analysis, carbamate bond reversibility, morphology, water vapour adsorption capacity in dynamic

regime and thermal, dielectric and mechanical behaviour. Considering the purpose of using these materials as capacitive pressure sensors, the change in their relative capacitance when different forces were applied was analysed. Biocompatibility through in vitro studies and antimicrobial activity were also evaluated.

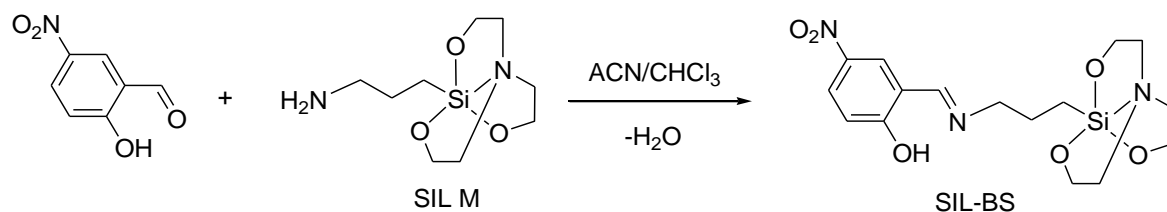
CHAPTER VII contains the general conclusions referring to the most important results obtained experimentally.

ORIGINAL CONTRIBUTIONS

CHAPTER II - SILATRAN DERIVATIVES

II.2. 1-(5-nitrosalicyliminopropyl)silatrane derivative (SIL-BS) obtaining

By the condensation reaction of 1-(3-aminopropyl)silatrane, SIL-M, with 5-nitrosalicylaldehyde in a molar ratio of 1:1 (**Scheme 2.14.**) in an acetonitrile/dichloromethane mixture, the 1-(5-nitrosalicyliminopropyl)silatrane derivative (**SIL-BS**) was obtained.



Scheme 2.14. Obtaining reaction of **SIL-BS** silatrane derivative

The product was isolated in crystalline state by slow evaporation of solvents at room temperature. It was characterized by elemental analysis, spectral methods (FT-IR, NMR, UV-Vis) as well as single crystal X-ray diffraction.

II.3.3 UV-Vis Spectroscopy

The presence of the hydroxyl group in the ortho position in the structure of the **SIL-BS** derivative may favor the formation of intramolecular hydrogen bond interactions, such as O-H---N and O---H-N, thus the occurrence of keto-enol tautomerism [139]. To highlight this phenomenon, UV-vis spectra were recorded in solvents with different polarities: THF, dichloromethane (DCM), methanol, acetonitrile (ACN) and DMSO, the keto-enolic tautomerism being also dependent on the H-bonding capacity of the solvent, the presence and polarity of the substituents (in this case, the nitro group). Thus, the UV-Vis electronic absorption spectra, recorded in all the solvents presented,

showed the coexistence of keto-enol tautomers: enol form (electronic transitions $S_1 \leftarrow S_0 (\pi^*, \pi)$) at 367 nm and keto tautomer (electronic transitions $S_1 \leftarrow S_0 (\pi^*, \pi)$) at 410 nm. The position of the absorption maxima found in DMSO changed when lower polarity solvents were used. Thus, in DCM the positions of the maxima were found at 356 nm (enol tautomer) and 408 nm (keto tautomer), respectively, while in methanol a hypochromic shift of the absorption maxima was observed, depending on the relative permittivity of the solvent (**Figure 2.9**).



Figure 2.9. UV-Vis spectra of **SIL-BS** compound in solvents with different polarities showing keto-enol tautomerization

II.3.4. Single crystal X-ray diffraction

X-ray diffraction revealed that the Schiff base **SIL-BS** has a crystalline molecular structure consisting of neutral [L] entities (**Figure 2.10**) and co-crystallised water molecules in a 1:1 ratio. The compound crystallizes in the chiral non-centrosymmetric space group ($C2/c$) in the monoclinic system. The molecular structure determined by single crystal X-ray diffraction confirms the keto-amine form (solid state). The hydrogen atom H2 is located closer to N2 than to the oxygen atom O6. The C16-O6 and C10-N2 bond distances confirm the tautomerism of enol-imine and keto-amine. Analysis of the structural data shows that the O6-C16 (1,241(9)Å) distance is shorter than distances found for C-OH in some similar compounds 1,2981(3), 1,342 (4), 1,351 (5)Å [132,133].

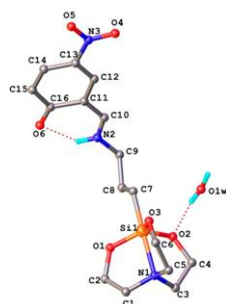


Figure 2.10. Asymmetric unit in the molecular structure of the **SIL-BS** compound determined by X-ray diffraction

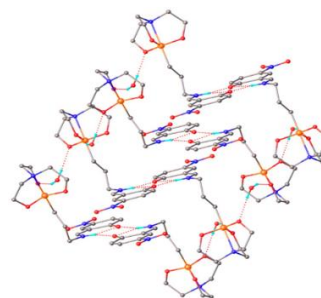


Figure 2.11. 1D supramolecular chain in the crystal structure of the **SIL-BS** compound formed by intermolecular hydrogen bonds $N-H \cdots O$ și $O-H \cdots O$

Bonding angles N2-C10-C11 (127,9(6)Å) and C10-N2-C9 (124,9(5)Å) are consistent with sp² hybridization of C10 and N2 atoms [141]. The amine group acts as a donor to the oxygen atom of the keto group. The molecular structure is stabilised by a hydrogen bond N2–H2A•••O6 resulting in the formation of a six-atom ring with bond length N2-H2•••O6 of 2,698(7)Å and angle of 131,2°, thus locking the molecular conformation and eliminating conformational flexibility. Intermolecular interactions such as N–H•••O and Ow-Hw•••O (**Figure 2.11.**) stabilizes the packaging.

II.4.2. Cell culture study

The effect of adding **SIL-SB** and its precursor **SIL M** on cell viability was analyzed after 48 h using two human carcinoma cell lines, hepatocarcinoma (HepG2 cells) and mammary adenocarcinoma (MCF7 cells). The XTT assay showed that **SIL M** has good compatibility with HepG2 and MCF7 cells even at the highest concentration tested (300 µg/mL) (**Figures 2.12. A and B**). The viability of HepG2 cells was reduced by about 20% when treated with 75 µg/mL **Sil-BS**, compared to control and **SIL M**-treated cells and showed a gradual decrease after this concentration (\approx 50% to 150 µg/mL and over 80 % at 300 µg/mL, $p < 0,0001$) (**Figure 2.12. A**). On the other hand, **SIL-BS** reduced the viability of MCF7 cells from 18,75 µg/mL compared to the **SIL M** corresponding concentration ($p < 0,001$), with a dramatic decrease observed at higher concentrations compared to both control and **SIL M** treated cells (more than 70% for concentrations in the range 75 ÷ 300 µg/mL, $p < 0,0001$) (**Figure 2.12. B**). Also, the graphical representation of the percentage of inhibition to log₁₀ **SIL-BS** (µg/mL) revealed that **SIL-BS** induced a greater inhibitory effect on the viability of MCF7 tumor cells, the inhibitory concentration, IC₅₀, being 65 µg/mL (**Figure 2.12. D**), compared to the IC₅₀ of 150 µg/mL on HepG2 (**Figure 2.12. C**). The cytotoxicity induced by the concentrations of **SIL-BS** and **SIL M** compounds, i.e. 9.37 and 150 µg/mL, on HepG2 and MCF7 cells was also examined by the live/dead cell assay, which consists of staining live cells green (calcein-AM) and dead cells red (propidium iodide) (**Figure 2.12. E**). Data from live/dead cell studies are consistent with XTT results and confirm a higher sensitivity of MCF7 cells to **SIL-BS** treatment than HepG2 cells. **SIL M** had no cytotoxic effects on HepG2 and MCF7 cells, but **SIL-BS** at 150 µg /mL induced high toxicity on HepG2 and MCF7 cells, with a more pronounced effect on MCF7 cells (**Figure 2.12. F and G**). The nitro group can undergo enzymatic reductions leading to reactive species and inducing therapeutic effects. Recently, nitro compounds have demonstrated anticancer activity through hypoxia-induced effects due to their bioreductive activation capacity, usually mediated by nitroreductases. The nitroreduction process involves the formation of the

nitrozo derivative, useful in the EPR effect on tumour cells, as an intermediate for compounds with primary amino groups (*Scheme 2.15.*) [149].

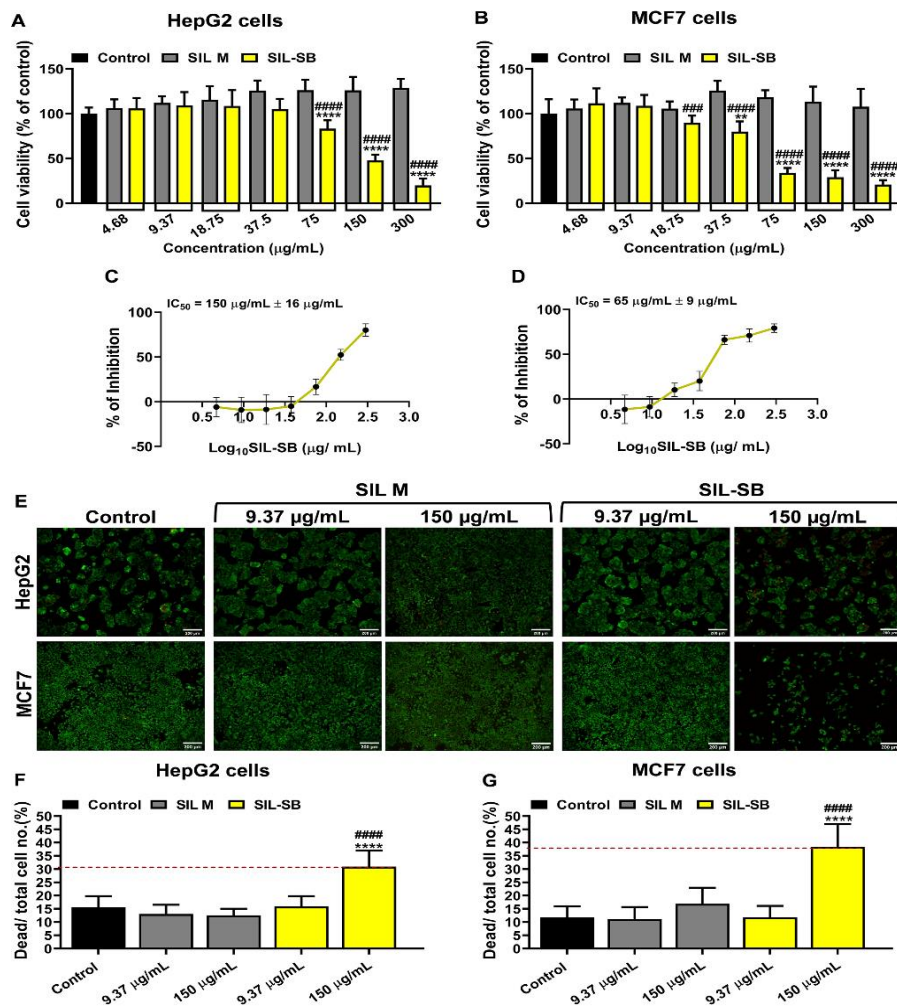
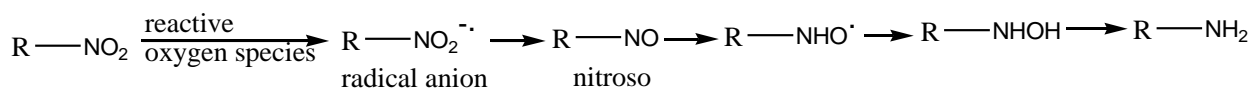


Figure 2.12. The viability of HepG2 (A) and MCF7 (B) cells, assessed by XTT assay. Dose response curves used to determine IC₅₀ of SIL-SB for HepG2 (C) and MCF7 (D) cells. Cells were treated for 48 hours with increasing concentrations (4.68 µg/mL to 300 µg/mL) of SIL M or SIL-SB. Merged Live/Dead cell images of HepG2 and MCF7 cells exposed to SIL M and SIL-SB for 48 hours (E). Live cells were stained with calcein AM (green) and dead cells are detected with propidium iodide (red). Scale bar: 200 µm. The percentage of the dead to total cell number determined by Live/Dead cell assay for HepG2 (F) and MCF7 (G). Statistical significance: **p < 0.01, ***p < 0.001 vs. control and ####p < 0.0001 vs. corresponding SIL M.



Scheme 2.15. The bioreductive pathway of nitro group

II.4.3.4. Molecular docking

Computational simulations related to molecular docking were performed using the AutoDock VINA algorithm [158] contained in the YASARA program [159-161]. As receptors for molecular docking, human serum albumin (HSA) and the major COVID-19 protease (M^{PRO}) have been used in this study. In this respect, the structures of the HSA and M^{PRO} were downloaded from the

protein database (<https://www.rcsb.org/>). Binding modes of ligand-receptor complexes were evaluated in terms of relative binding energies (E_b , kcal/mol) and dissociation constants (K_d , μM). Typically, lower values of these estimates indicate stronger receptor-ligand interaction. Finally, the molecular docking results were subjected to cluster analysis by adopting a root mean square deviation (RMSD) tolerance of 5,0 Å. Computational results showed that doped complexes HSA@SIL M (**Figure 2.17.**) and HSA@SIL BS (**Figure 2.18.**) were stabilized by hydrophobic interactions. Values of affinity estimators (relative energy E_b and dissociation constant K_d). As reported, the number of contact residues was equal to 14 and 12, for **SIL-M** and **SIL-BS** ligands. The dissociation constant is obviously low ($K_d=0.148 \mu\text{M}$) for the HSA@SIL BS docked system, compared to the HSA@SIL M docked complex ($K_d=3.345 \mu\text{M}$). According to these computational data, **SIL-BS** is shown to have interacted much more strongly with the receptor (HSA), compared to the **SIL M** ligand.

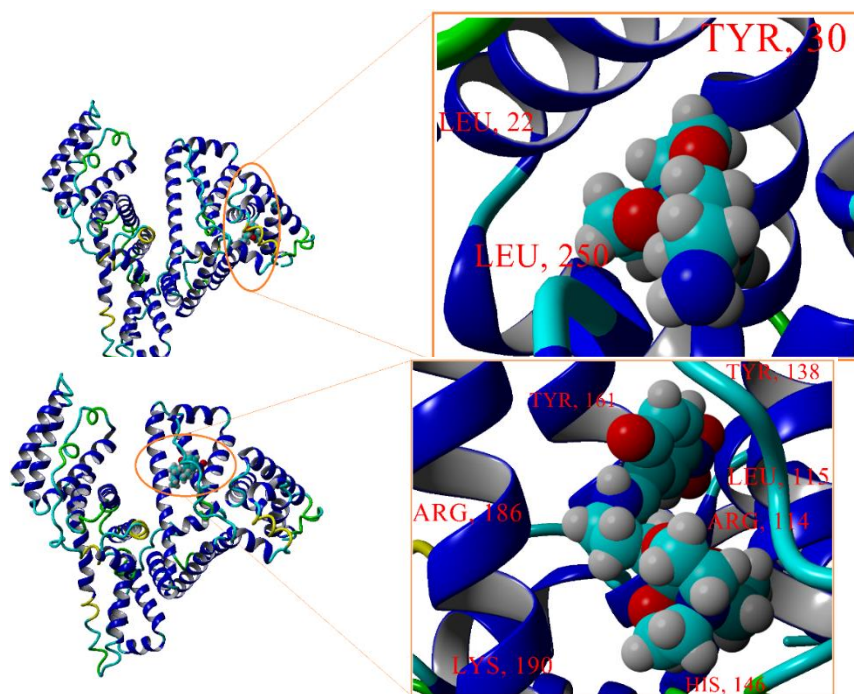


Figure 2.17. Molecular rendering of the best docked pose showing the interaction between HSA (receptor) and **SIL M** ligand; global docking view and zoom image)

Figure 2.18. Molecular rendering of the best docked pose showing the interaction between HSA (receptor) and **SIL-BS** ligand; global docking view and zoom image)

II.4.5. Antimicrobial activity

The antimicrobial activity of the compounds was evaluated on three fungal species *Aspergillus niger* ATCC-16888, *Fusarium* ATTC-20327, *Penicillium chrysogenum* ATCC-11709 and two bacteria *Bacillus* sp. ATCC-19986, *Pseudomonas aeruginosa* ATCC-27853, provided by the American Type Culture Collection (ATCC), SUA. *In vitro* studies were carried out by the MIC test method according to standard procedures (SR-EN 1275:2006 and NCCLS:1993).

Table 2.3. Results of antimicrobial activity of tested compounds **SIL M** and **SIL BS**

Sample	MIC ($\mu\text{g/ml}$)				
	Fungi			Bacteria	
	<i>Aspergillus fumigatus</i>	<i>Penicillium frequentans</i>	<i>Fusarium</i>	<i>Bacillus sp.</i>	<i>Pseudomonas sp.</i>
SIL M	1.20 \pm 0.02	1.20 \pm 0.01	1.21 \pm 0.01	2.80 \pm 0.01	2.90 \pm 0.11
SIL-BS 1 %	2.08 \pm 0.21	1.90 \pm 0.12	2.08 \pm 0.11	4.04 \pm 0.21	4.08 \pm 0.24
SIL-BS 25 %	>32	> 32	> 32	>256	>256
Caspofungin^b	0.72 \pm 0.01	0.72 \pm 0.01	0.72 \pm 0.01	-	-
Kanamycin^b	-	-	-	1.8 \pm 1.11	1.6 \pm 0.98

The emergence of pandemic transmissible SARS-CoV-2 infection caused by the COVID-19 virus has led to the development of new antiviral agents that are well tolerated by people with associated diseases: cancer, hypertension, respiratory infections, diabetes, etc. Current treatment options for SARS-CoV-2 consist of traditional Chinese medicine combined with effective drugs for SARS-CoV-1 and MERS-CoV (Chloroquine and Lopinavir/Ritonavir), which have been evaluated in clinical trials and some have received FDA approval for administration. In addition to specific antiviral activity, these drugs must first have a minimal risk of side effects, as well as a high binding affinity for target plasma proteins ensuring high bioavailability [169]. In view of the above and given the water solubility, high biocompatibility and very good antimicrobial activity of 1-(3-aminopropyl)silatran (SIL M), its antiviral capacity was tested by molecular docking simulations on M^{PRO} (COVID-19 main virus protease) (PDB id: 6LU7 (<https://www.rcsb.org/structure/6LU7>)). SARS-CoV-2 is an RNA virus with four structural proteins: the capsid, sheath, membrane and nucleocapsid. The main protease (M^{PRO}) is a cysteine- protease of 33,8 kDa. This plays an essential role in the viral activity that ensures virus replication, so its inhibition may be a target for antiviral drug development [170]. A number of approved antiviral agents such as Remdesivir, Chloroquine and Hydroxychloroquine have been shown to be effective against SARS-CoV-2 infection. Comparative docking studies showed that Remdesivir has the highest binding affinity to M^{PRO} with an Eb = -7.17 kcal/mol, followed by Hydroxychloroquine and Chloroquine with similar Eb of -6.68 kcal/mol and -6.47 kcal/mol, respectively [170].

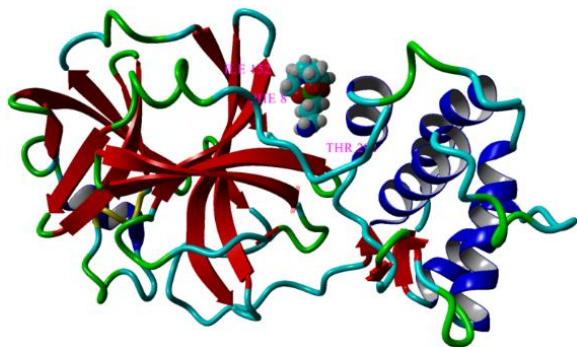


Figure 2.19. Molecular rendering of the best docked pose showing the interaction between M^{PRO} receptor (COVID-19 main protease) and silatran SIL M

The silatran compound **SIL M** was also shown to be effective in inhibiting M^{PRO} , $E_b = -5.794$ kcal/mol being close to that of compounds with demonstrated inhibitory activity in clinical trials and granted marketing approval. Simulation results showed that the docked $M^{PRO}@SIL M$ complex was stabilized by hydrophobic interactions (**Figure 2.19.**), and silatran (**SIL M**) contacted 14 residues in the receptor. For this case, the affinity estimators were equal to $E_b = -5.794$ kcal/mol and $K_d = 56.61 \mu M$.

CHAPTER III - MODIFIED MESOPOROUS SILICA

III.2. Preparation of mesoporous silica (MS) particles

In situ modified mesoporous silica particles with organic and/or functional groups were prepared by a previously reported procedure [196], consisting of co-condensation of tetraethylsilicates (TEOS) with trialkoxysilanes (TAS) containing the desired organic groups ($-(CH_2)_3-NH_2$, or $-CH_3$) or TEOS homocondensation, in aqueous basic medium (NaOH), and in the presence of the surfactant cetyltrimethylammonium bromide (CTAB) in low concentration (**Figure 3.20.**). The working protocol [196] consists of forming a mixture of surfactant (CTAB) (2 g) and NaOH solution (7 mL 8% sol in water) in distilled water (480 mL), heating this mixture for 30 min at 80 °C with stirring, followed by addition of TEOS and TAS in the predetermined ratio and resuming heating for another 2 h under the same conditions. The silica formed is isolated by filtration, washed with water and methanol and dried at 80°C under vacuum for 18 h.

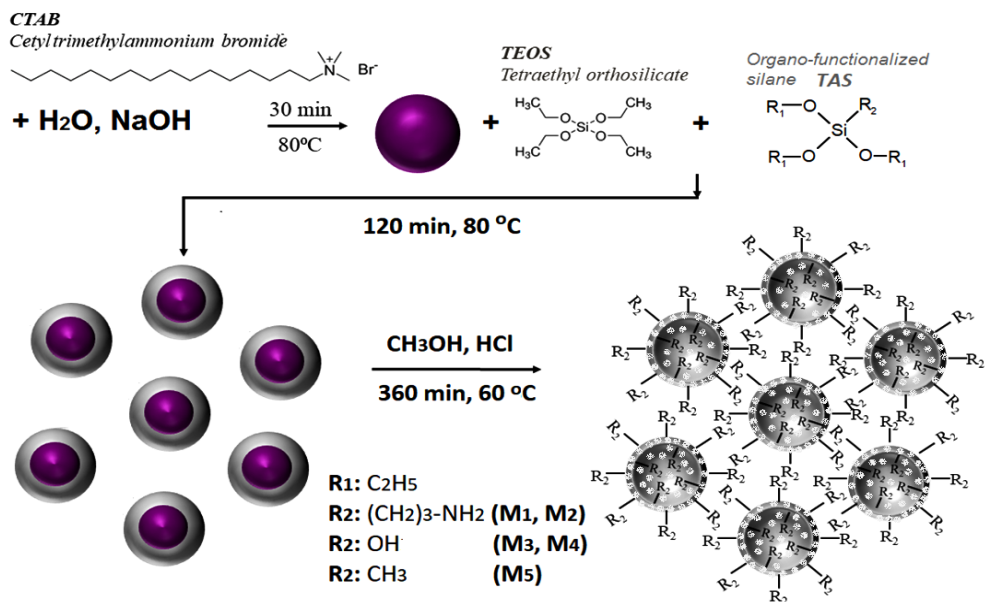


Figure 3.20. Schematic representation of the preparation protocol of *in situ* surface organo-modified and/or functionalized silica particles

For pore release/activation, the material is extracted in a mixture of concentrated hydrochloric acid and methanol (1mL: 100 mL per 1 g of dry material) at 60 °C for 6 hours, after which the surfactant-released product is washed with water and methanol and dried again under vacuum. TAS was mixed with (3-aminopropyl)triethoxysilane (APTES) leading to the formation of **M1** and **M2** silicas with NH₂ groups on the inner and outer surfaces or with triethoxymethylsilane (MTES), leading to the formation of **M5** silica, while samples **M3** and **M4** were obtained by homocondensation of TEOS, generating Si-OH groups on the surface.

Table 3.5. The main characteristics of the organo-modified and/or functionalized silica particles

Sample	M1	M2	M3	M4	M5
Surface group	-(CH ₂) ₃ NH ₂	-(CH ₂) ₃ NH ₂	-OH	-OH	-CH ₃
Pore size (nm) ^a	3.33	3.02	3.06	3.04	2.49
BET area (m ² /g)	722	621	1001	936	943

III.2.1. DOX loading in mesoporous silica (samples D1-D5)

Loading experiments were performed at room temperature, pH 7.4 (0.1% PBS solution). Approximately 10 mg MS were dispersed in 4 mL 0.1% DOX solution. The mixture was subjected to ultrasonic treatment for 30 seconds, after which it was shaken overnight in a rotary shaker at room temperature under dark conditions. The next day, the loaded silica was centrifuged, the supernatant

was separated and analyzed by UV-vis to determine by difference the degree of loading of the silica with DOX. The loaded silica was washed with distilled water and dried under dark conditions (**Figure 3.21**). The concentration of DOX in silica was calculated based on the molar extinction coefficient of DOX in PBS 7.4 ($\epsilon=5498 \text{ M}^{-1}\text{cm}^{-1}$ at $\lambda_{\text{max}}=482 \text{ nm}$).

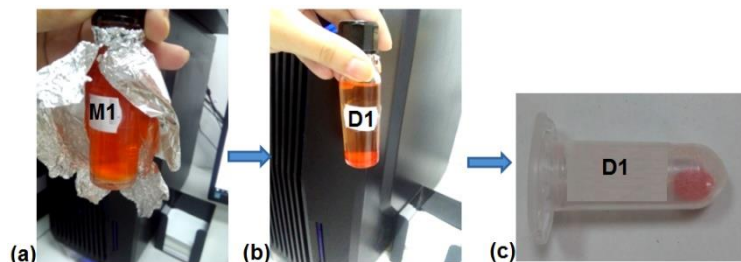


Figure 3.21. The color changes during the loading of DOX: (a) **M1** in DOX solution, (b) **D1** in DOX solution, (c) **D1** in dried state

The encapsulation efficiency (EE %) and loading capacity (LC) were calculated using the formulas:

$$EE(\%) = \frac{W_{(drug\ in\ silica)}}{W_{(initial\ added\ drug)}} \times 100 \quad (1)$$

$$LC = \frac{W_{(drug\ in\ silica)}}{W_{(silica)}} \quad (2)$$

where $W_{(drug\ in\ silica)}$ is the amount of DOX in MS sample calculated by the differences between the initial DOX amount and the DOX in supernatant after loading process, $W_{(initial\ added\ drug)}$ is the amount of the DOX in the stock DOX solution 0.1 % used for loading experiments and $W_{(silica)}$ is the mass of silica (mg) used for encapsulation process. The calculated values for EE % and LC are shown in **Table 3.6**.

Tabelul 3.6. Loading of DOX in terms of EE % and LC in the MS particles

Sample	EE, %	LC, $\mu\text{g}/\text{mg}$
M1	16.75	6.7
M2	14.13	5.65
M3	81.80	32.7
M4	78.74	31.49
M5	90	36

III.3.1. FTIR Spectroscopy

FTIR spectroscopy was used to investigate the spectral changes that occurred in MS as a result of DOX loading. IR spectra of MS, before and after DOX encapsulation, revealed the presence of stretching vibrations characteristic of Si-O bonds at 1062 cm^{-1} and 960 cm^{-1} , N-H and

O-H at $3400\text{--}3440\text{ cm}^{-1}$, C-H at $2920\text{--}2855\text{ cm}^{-1}$, of the deformation and bending specific to C-H bonding at 1464 and 1416 cm^{-1} [197].

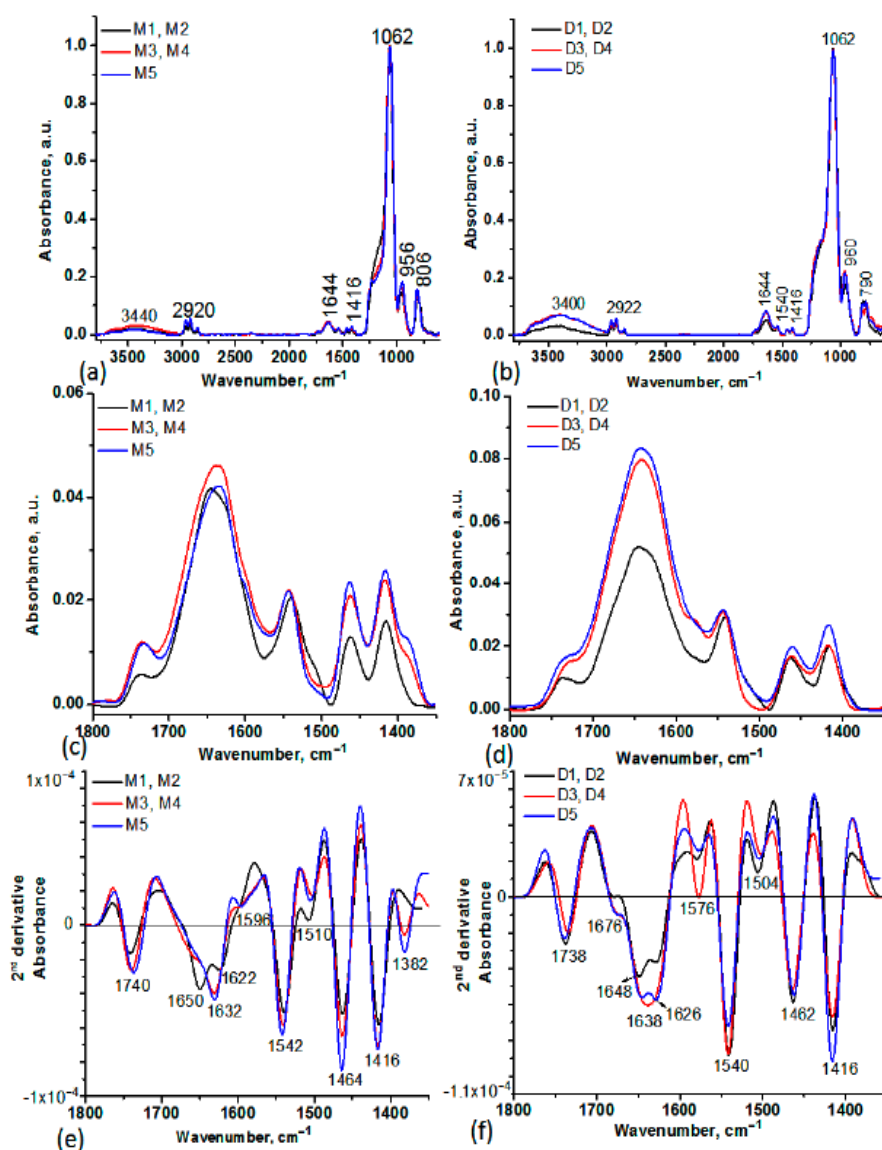


Figure 3.22. FT-IR spectra in absorbance of MS before (**M1-M5**) (a) and after (**D1-D5**) (b) DOX encapsulation. Spectral details in the $1800\text{--}1400\text{ cm}^{-1}$ spectral range of MS before (**M1-M5**) (c) and after (**D1-D5**) (d) DOX encapsulation, where “M” denoted the MS samples before DOX loading and “D” denoted the MS samples after DOX loading. The 2nd derivative of the IR spectra in the $1800\text{--}1400\text{ cm}^{-1}$ spectral range of MS before (**M1-M5**) (e) and after (**D1-D5**) (f) DOX encapsulation. The negative bands in the 2nd derivative spectra correspond to the maxima of absorbance spectra in the same spectral region

III.4. DOX release studies from silica

To investigate kinetic release patterns, the release profiles obtained were analysed by three models (Higuchi, Korsmeyer-Peppas and Peppas-Sahlin).

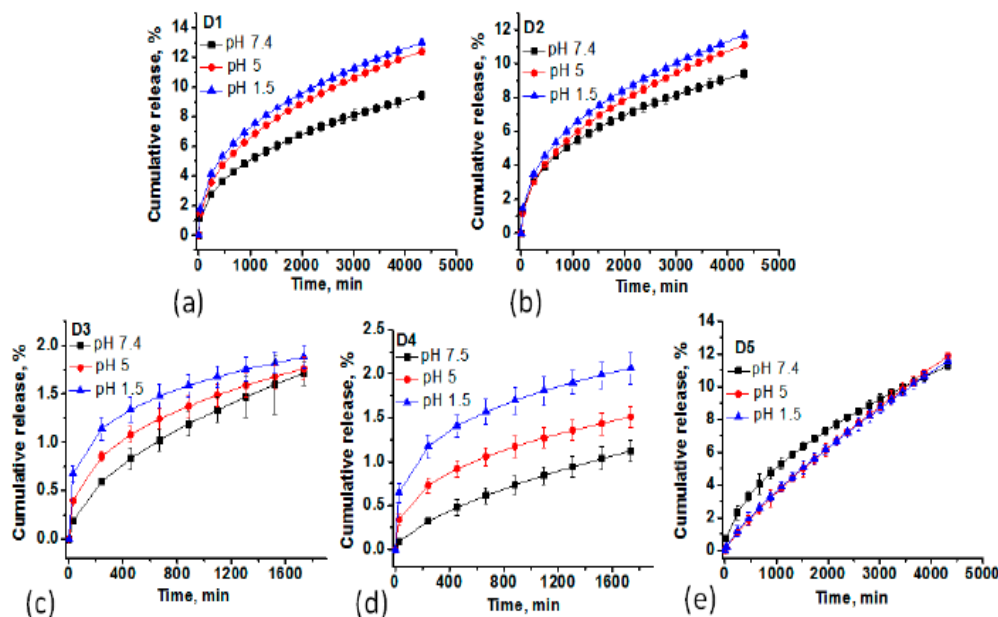


Figure 3.27. The Cumulative Release (%) of DOX during 72 h at pH 1.5, 5, and 7.4 for D1 (a), D2 (b), D3 (c), D4 (d), and D5 (e) fitted with Krosmeeyer–Peppas kinetic model

The diffusion coefficient values for all samples except **D5** are close to 0.43, supporting a Fickian diffusion (diffusion mechanism dependent release). For **D5**, the value of n is $0.43 < n < 0.83$, supporting an anomalous transport, a release dependent on swelling, degradation or relaxation of the matrix. A higher rate constant, K , was found for samples **D1** and **D2**, where DOX was mainly bound at the surface. The results reported in this chapter are similar to those reported in the literature for some complex release systems, and our perspectives are directed towards optimizing release conditions, taking into account the cumulative influence of different factors: porosity, cellulose dialysis membrane, pH, temperature, ultrasound, release time, etc. Silica particles are biocompatible, with a hydrolysis rate of 76% in 56 days and excretion through the urinary tract. By internal drug loading, silica materials are able to provide prolonged effective concentration [210].

III. 5. Evaluation of the biomedical application potential of functionalized mesoporous silica

In the present study, the cytotoxicity of MS samples before and after DOX encapsulation was investigated on three cell lines, HGF (normal cell line) and two cancer cell lines (MCF-7 and HeLa). Investigation of MS compatibility on the normal cell line at a concentration of 30 $\mu\text{g}/\text{mL}$ revealed moderate biocompatibility for **M1**, **M2** and **M3** samples (viability is less than 80%). The relatively lower cytotoxicity on normal cells could be explained by silica functionalization involving a strong interaction with cells, followed by its internalization which favors apoptosis [217]. The IC_{50} values of

D1 were 136.5 $\mu\text{g/mL}$ on HeLa and 73.98 $\mu\text{g/mL}$ on MCF-7, corresponding to an encapsulated DOX concentration of 0.90 $\mu\text{g/mL}$ on HeLa and 0.49 $\mu\text{g/mL}$ on MCF-7, respectively (**Figure 3.28.a**).

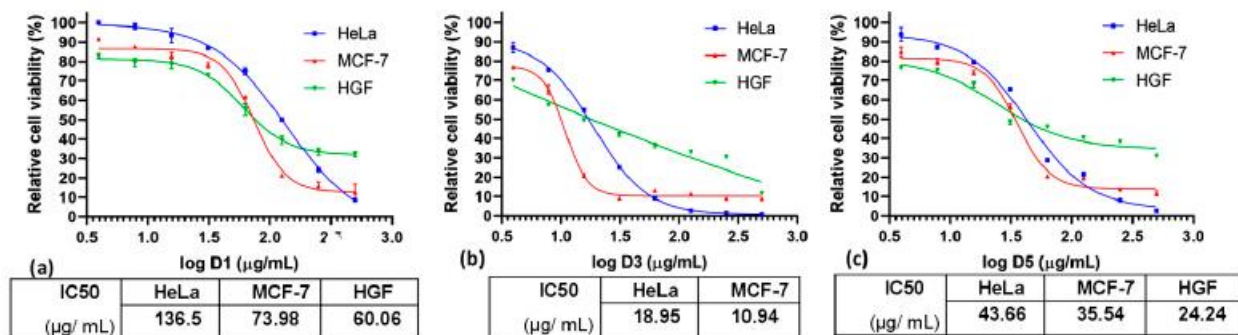


Figure 3.28. Cytotoxicity of the DOX-loaded MS samples: (a) D1, (b) D3, and (c) D5 on HeLa, MCF-7, and HGF cell lines. Relative IC₅₀ values were determined by non-linear regression variable slope with four parameters using the Graphpad Prism software. All data are presented as the mean with standard deviation from three independent experiments

III.5.3. Evaluation of bio- and mucoadhesion of functionalized mesoporous silica

Given that a large number of drugs are administered on different mucosae, the bio- and mucoadhesive properties of silica particles have been investigated. Bioadhesion of MS samples was tested at pH 7.4 at 37 °C. Mucoadhesion tests were performed on different tissues: stomach, small and large intestine and colon, in simulated physiological medium with a temperature of 37 °C and PBS media with different pH values ranging from 1.5 to 8.5, depending on the tissue region concerned. (**Figure 3.29**).

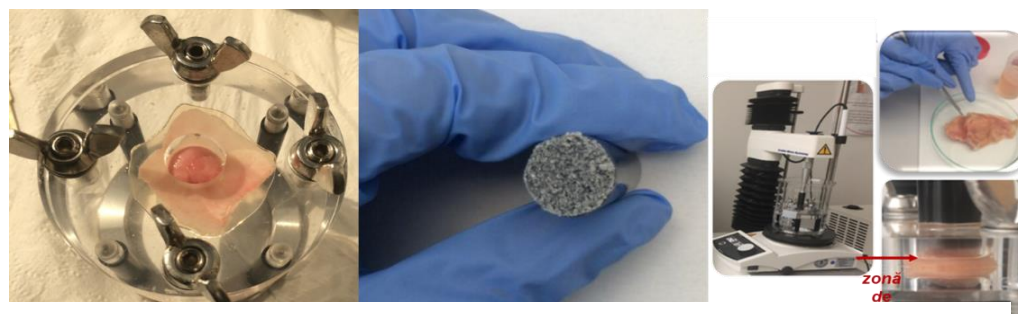


Figure 3.29. Images of mucoadhesion registered during mucosal preparation and MS assessment

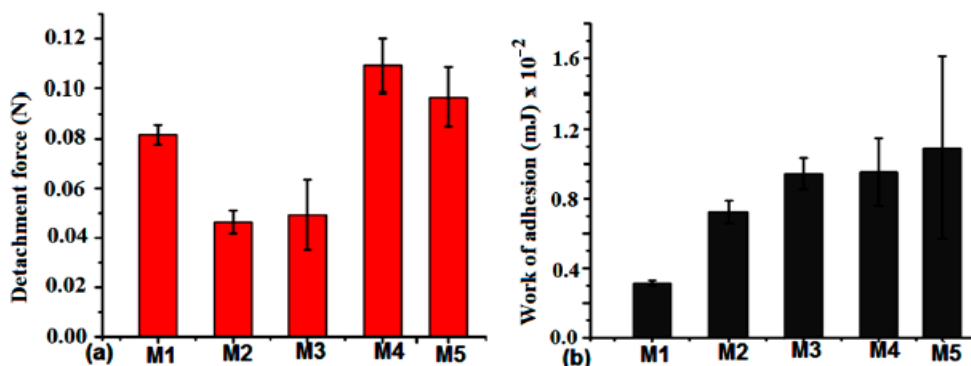


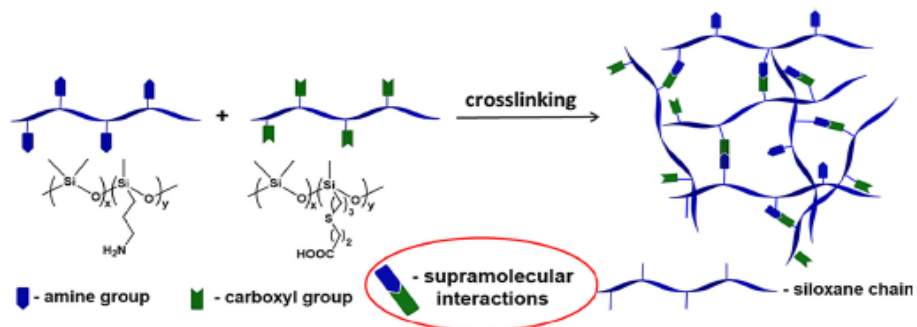
Figure 3.30. The detachment force (a) and the work of adhesion (b) of the MS samples on a synthetic membrane substrate

Bioadhesion of MS samples on a synthetic cellulose membrane revealed a strong interaction of **M3** and **M4** samples facilitated by the presence of hydroxyl groups on the surface. The detachment force was higher for samples **M1** and **M4** (**Figure 3.30.a**), while the work of adhesion was higher for samples **M3** and **M4** (**Figure 3.30.b**). The presence of amino and hydroxyl groups on the surface of silica particles explains the adhesion phenomenon for these samples. The variation in detachment force within the same functional groups may be due to their different concentration in contact with the membrane. In the large intestine and colon segments, almost all samples have similar values, comparable to those found for the stomach mucosa. Mucoadhesivity studies of silica particles are essential for understanding the safety profile when administered locally, as these particles can accumulate becoming toxic to the body. Thus, the process of elimination and degradation depends on size, surface functionalisation, loading, etc. It has been shown that larger particles are eliminated mainly via the gastrointestinal tract, while smaller particles are eliminated via the urinary tract. The biodegradation process of these particles occurs mainly by hydrolysis, with silanes being the main degradation products. Intestinal mucoadhesion is also important for pH-dependent release and adsorption of some silica-loaded drugs when administered orally or intraperitoneally [226,227].

CHAPTER V. SUPRAMOLECULAR SILICONE NETWORKS

V.2.1. Obtaining supramolecular silicone networks based on functionalized polysiloxanes (SN1-SN3)

In a first approach, polysiloxanes with pendant amino groups were cross-linked by mixing with another polysiloxane having carboxyl groups attached (**Scheme 5.17**). Thus, a polysiloxane functionalized with amino groups, namely 6.4 mol% units of 3-aminopropylmethylsiloxane (**PDMS-NH₂-1**) was cross-linked by combining in different mass ratios (0.5/0.25; 0.5/0.375; 0.5/0.5) with a laterally functionalized polysiloxane- α,ω -diol with 14.9 mol% carboxypropyl groups (well below 100% as used in the literature [284]), **PDMS-COOH** resulting in samples **SN1**, **SN2** and **SN3**, respectively (**Table 5. 18**). To ensure their good miscibility, an addition of solvent (THF) was used for a concentration of about 50%, and the mixtures were homogenized with a SpeedMixer, after which they were processed into films, and left for cross-linking and solvent evaporation for 24 h at room temperature and 72 h at 70 °C in a vacuum oven. Colorless, transparent soft films with smooth morphology were obtained, both on the surface and in section.

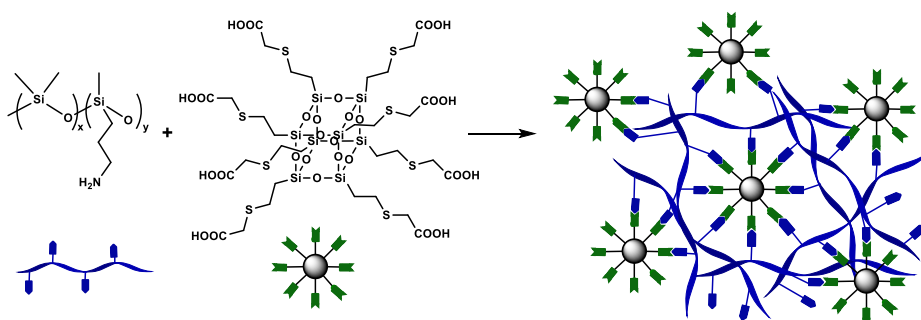


Scheme 5.17. Formation of supramolecular networks based on **PDMS-NH₂** and **PDMS-COOH** (samples SN1-SN3)

Table 5.18. Reagents and feed amounts for the supramolecular networks preparation

Sample	Polimer matrix		Crosslinker		NH ₂ :COOH molar
	PDMS-NH ₂	g polimer/mL THF	Substrate-COOH	g/mL THF	
SN1	PDMS-NH ₂ -1	1.50/2.0	PDMS-COOH	0.50/1.0	1:0.7
SN2	PDMS-NH ₂ -1	0.50/0.5	PDMS-COOH	0.25/0.5	1:1.1
SN3	PDMS-NH ₂ -1	0.50/1.0	PDMS-COOH	0.375/1.0	1:1.7
SN4	PDMS-NH ₂ -2	0.75/0.5	POSS-COOH	0.075/0.5	1:0.5
SN5	PDMS-NH ₂ -1	0.75/2.5	POSS-COOH	0.075/2.5	1:0.7

V.2.2. Obtaining supramolecular silicone networks based on functionalized polysiloxanes and oligosilsesquioxanes (SN4, SN5)



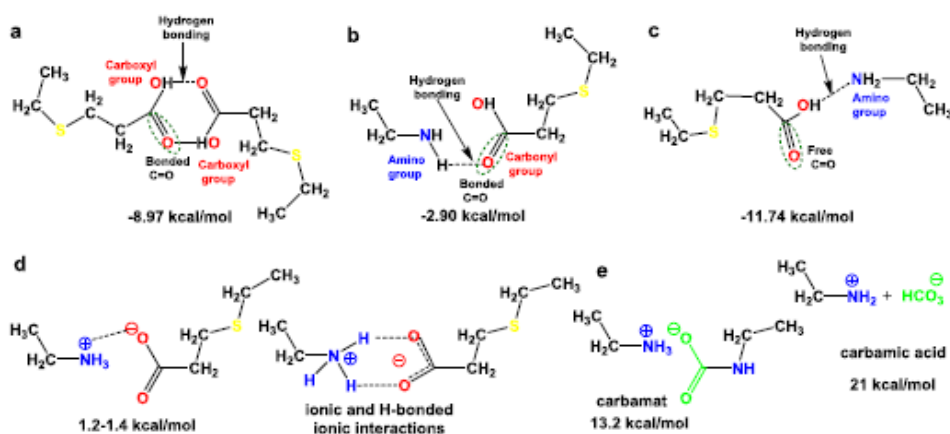
Scheme 5.18. Formation of supramolecular networks based on **PDMS-NH₂** and **POSS-COOH** (samples SN4, SN5)

In another approach, siloxanes functionalized with amino groups on the chain were cross-linked with a polysilsesquioxane functionalized with carboxyl groups, **POSS-COOH** (Scheme 5.18.). **PDMS-NH₂-2** and **PDMS-NH₂-1** with different amino group contents (6.4 and 9.8 mol%, respectively) were mixed in the same mass ratio, 10:1 **PDMS-NH₂:POSS-COOH**, in minimal

amounts of THF as solvent to ensure good dissolution of solid **POSS-COOH** and mixing with **PDMS-NH₂**.

V.3.1. Structural characterisation of supramolecular networks

By mixing the two types of precursors it is expected that initially hydrogen bonds are established between the amino and carboxyl groups (**Scheme 5.19.a-c**) [284], gradually increasing the viscosity due to proton transfer from the carboxyl group to the amino group, resulting in the formation of ionic bonds (**Scheme 5.19.d,e**) [283,286], favoured by the non-polar environment created by the dimethylsiloxane fragments.



Scheme 5.19. Supramolecular interactions possible to be established in prepared silicone networks: (a) -COOH/-COOH groups; (b) =C=O/-NH₂ groups, (c) -OH/NH₂ groups [284], (d) NH₃⁺/COO⁻, (e) NH₃⁺/NHCOO⁻, NH₂⁺/HCO₃⁻ [288]

Network formation was first demonstrated by FTIR spectroscopy. The IR spectra of samples **SN1**, **SN2** and **SN3** revealed the presence of absorption bands corresponding to Si-O-Si bond stretching vibrations at 1080-1008 cm⁻¹, Si-CH₃ symmetric deformation vibrations at 1258 cm⁻¹ and Si-C group stretching vibrations at 862-790 cm⁻¹ (**Figure 5.39.a**). In addition to these, characteristic absorption bands for NH₂/NH₃⁺ and COOH/COO⁻ groups are also present. In the 1650-1500 cm⁻¹ spectral region, C-N bond stretching vibrations, asymmetric and symmetric deformation vibrations of NH₂ groups bound by intermolecular hydrogen bonding interactions, superimposed on COOH groups also self-assembled by hydrogen bonds, were highlighted. The bands from 1414-1398 cm⁻¹ are specific to bending and shearing vibrations of methylene groups, stretching vibrations of the C-O bond and deformation vibrations of O-H bonds. Also visible in the spectrum are absorption bands attributed to asymmetric and symmetric C-H bond vibrations and stretching at 2962 and 2902 cm⁻¹ respectively, asymmetric C-H bond deformation vibrations at 1488-1444 cm⁻¹ and out-of-plane N-H/O-H bond bending vibrations at 704-660 cm⁻¹ [287].

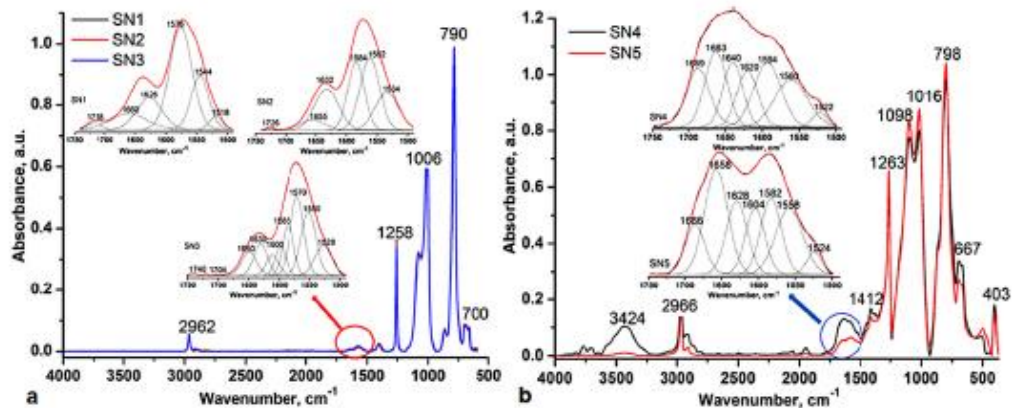


Figure 5.39. IR absorbance spectra of the supramolecular networks **SN1-SN3** (a) and **SN4-SN5** (b), - inset-spectral region 1750-1500 cm^{-1} , deconvoluted based on 2nd derivative of the spectra highlighting the H-bonded carbonyl and N-H vibrations in the supramolecular networks.

V.3.3. Thermal behaviour of supramolecular networks

The thermal behaviour of the prepared networks was analysed by TGA and DSC. In the first series, the main mass losses occurred at 327 (**SN1**), 403 (**SN2**) and 362 $^{\circ}\text{C}$ (**SN3**), indicating appreciable thermal stability (**Figure 5.43.**). In some cases, there were some losses (about 3-4 gr%) at low temperatures that can be attributed to the departure of traces of solvent or volatile fractions present in the two polymers. The presence of polar groups, mainly carboxylic, facilitates the breaking of the siloxane bond on heating, making the residual mass at 700 $^{\circ}\text{C}$ insignificant (2-5 gr%). The exception is sample **SN4**, which had a residual of 19%. All grids have a glass transition around -115 $^{\circ}\text{C}$, both at first and second heating. The exception is sample **SN4** whose T_g is slightly higher, -109 $^{\circ}\text{C}$ (**Figure 5.44.**), probably due to the existence of stronger interactions within the network, having a polymeric component with higher density of amino groups. This network also has the highest cumulative melting enthalpy value, 5,563 J/g at first heating, indicating a higher degree of crystallinity, compared to 1,275 J/g for **SN3**. The networks also show up to three melts at first heating (generally at positive temperatures, except for sample **SN2**, which shows melting at -43 $^{\circ}\text{C}$ characteristic of amorphous siloxane chain [291]), while some of them also have one or two melting points at second heating and one or two crystallizations on cooling. These are determined by the strength of ionic interactions [292], the density and distribution of intermolecular interactions that are established within the networks.

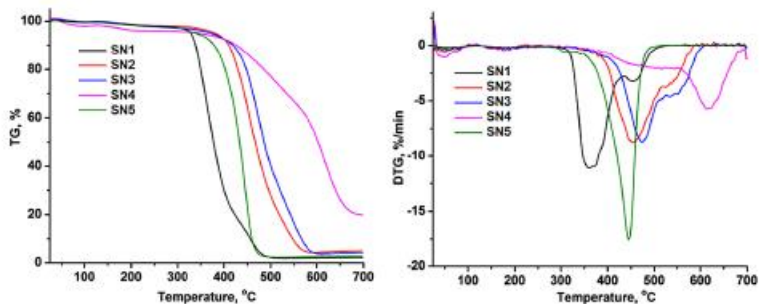


Figure 5.43. TG (left) and DTG (right) curves of the tested supramolecular networks

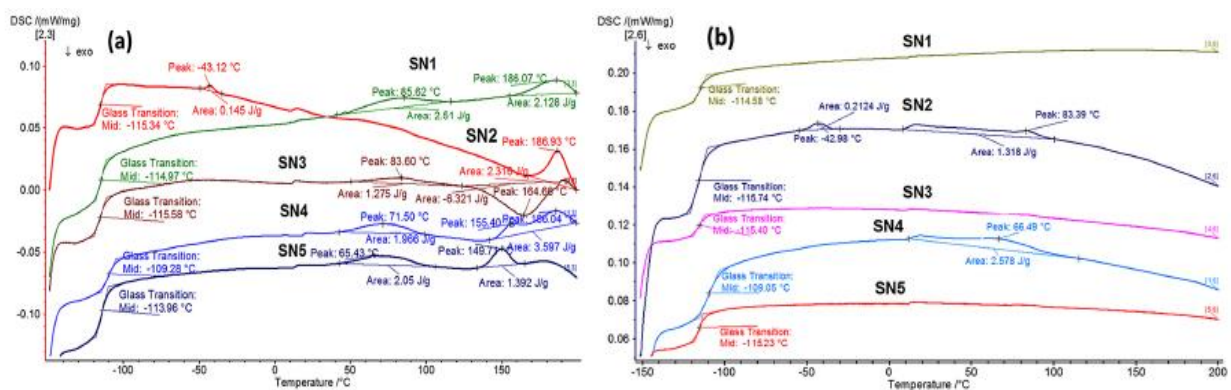


Figure 5.44. DSC curves on the first (a) and second (b) heating processes

V.3.4. Mechanical behaviour of supramolecular networks

The specimens were tested by linear and uniaxial cyclic tensile tests (10 cycles of stretch-pull for each film). Tensile strength and ultimate deformation were determined from stress-strain curves. Young's modulus values in the range 0 - 10% strain were also determined from these measurements. As can be seen from **Figure 5.45.**, the two types of networks behave very differently. Analysing the results presented in **Table 5.21.**, it can be seen that, in the case of **PDMS-COOH** cross-linked samples, the tensile strength and Young's modulus values increase with increasing carboxyl group content, while the elongation at break decreases. In a recent study [284] on a similar system, by DFT calculations correlated with IR studies, it was found that three types of hydrogen bonds are possible: between two carboxyl groups with an energy of -8.97 kcal/mol, between a carbonyl group and an amine group of -2.90 kcal/mol, between an OH group and an amino group of -11.74 kcal/mol (**Scheme 5.19.a,b,c**). As such, it can be assumed that when the precursor with COOH groups is added over the one with amino groups, supramolecular interactions between the carboxyl and amine groups are formed with priority.

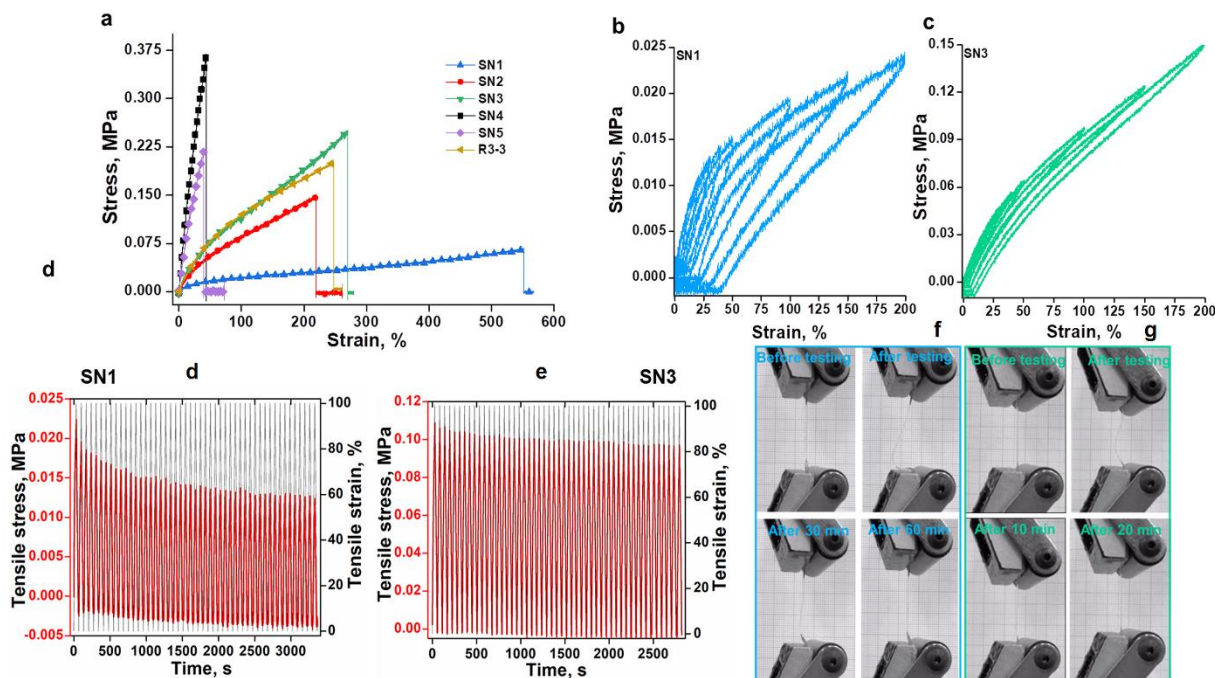


Figure 5.45. Relevant mechanical behavior for the supramolecular networks: (a) stress-strain curves of the supramolecular networks **SN1** - **SN5** as compared with that for covalent network **R3-3**; cyclic stress-strain curves for samples **SN1** (b) and **SN3** (c) and the corresponding stress relaxation stress relaxation presented by tensile stress (MPa) dependence as a function of time (s) (d,e); Evidence for the return of the ultrasoft network **SN1** (f) and the network **SN3** (g) from the elongated shapes by 200% to the original.

Table 5.21. The main mechanical parameters of the prepared supramolecular networks.

Sample	Young Modulus, at 10% strain, MPa	Strain at break (%)	Tensile strength (MPa)
R3-3	0.22	248	0.20
SN1	0.06	551	0.06
SN2	0.17	219	0.14
SN3	0.24	269	0.25
SN4	1.01	44	0.36
SN5	0.71	39	0.21

V.3.5. Study of the dielectric properties of supramolecular networks

As expected, the presence of polar and ionic groups induces a significantly increased dielectric permittivity (up to 22.5) at room temperature, depending on their content and ratio (**Figure 5.46.**, before sample heating), compared to that of the R3- 3 reference ($\epsilon' = 3.2$) based on polydimethylsiloxane covalently cross-linked by thiol-ene addition. As can be seen from **Figure 5.46.**, the dielectric permittivity has higher values in the low frequency range (due to the fast response of dipoles to the applied electric field [293,294]) but continuously decreasing in the case of **SN4** and **SN5** samples, or establishing a plateau at high frequencies due to the inability of

dipoles to orient to a faster field change [295]. The dielectric permittivity is determined by large dipole moments in molecules associated through physical (hydrogen or ionic) interactions [296]. In the case of these networks, IR studies have shown the presence of hydrogen bonds but also of ionic interactions, such as ammonium carbonate, carbamate and carbamic acid, whose formation is favoured by the non-polar nature of the medium created by the dimethylsiloxane fragments. The ionic association process is exothermic and occurs spontaneously at all temperatures.

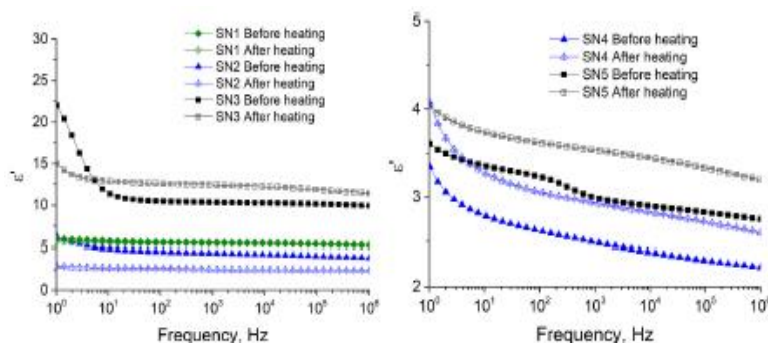


Figure 5.46. Comparative dielectric spectra showing the dielectric relaxation (ϵ') as a function of frequency of the pristine supramolecular networks at room temperature before and after heating to 150 °C

V.3.6. Self-repairing capacity of supramolecular networks

Due to cross-linking by hydrogen bonding or electrostatic interactions, the resulting materials are expected to respond to external stimuli such as temperature and pH [286] and exhibit self-repairing ability [297]. The development of silicone elastomers with self-repairing capability is of high importance due to their promising applications [281]. To test the self-repairing ability, the elastomeric film was cut into small pieces using a scalpel and then pressed between two glass plates. It can be seen (**Figure 5.47.a**) how, by pressing, the material regains the appearance of a continuous, transparent, uniform film. In another approach, the edges of two pieces of film cut with a scalpel were brought back into contact and left for a period of time at room temperature, restoring the unitary film (**Figure 5.47.b**), their repair being verified by mechanical stretching tests. The evolution of this process was followed by recording the stress-strain curves at different time intervals after contacting the cut pieces for sample **SN1** (**Figure 5.47.c**). As can be seen, after 10 days of contact at room temperature, 95% of the elongation at break is recovered at 30% of the initial stress. Similar to the adhesion process, the self-repair mechanism takes place in two stages, a contact stage and a consolidation stage of the networks involved. In the consolidation stage, the contribution of intermolecular interactions is major, followed by interdiffusion of polymer chains to promote prolonged adhesion [298]. In general, a repair process is mainly favoured by the flexibility of polymer segments, which facilitates interfacial diffusion and

the establishment of intermolecular interactions leading to network cross-linking. A high cross-linking density will lead to rigid networks with a lower self-repair capacity [286].

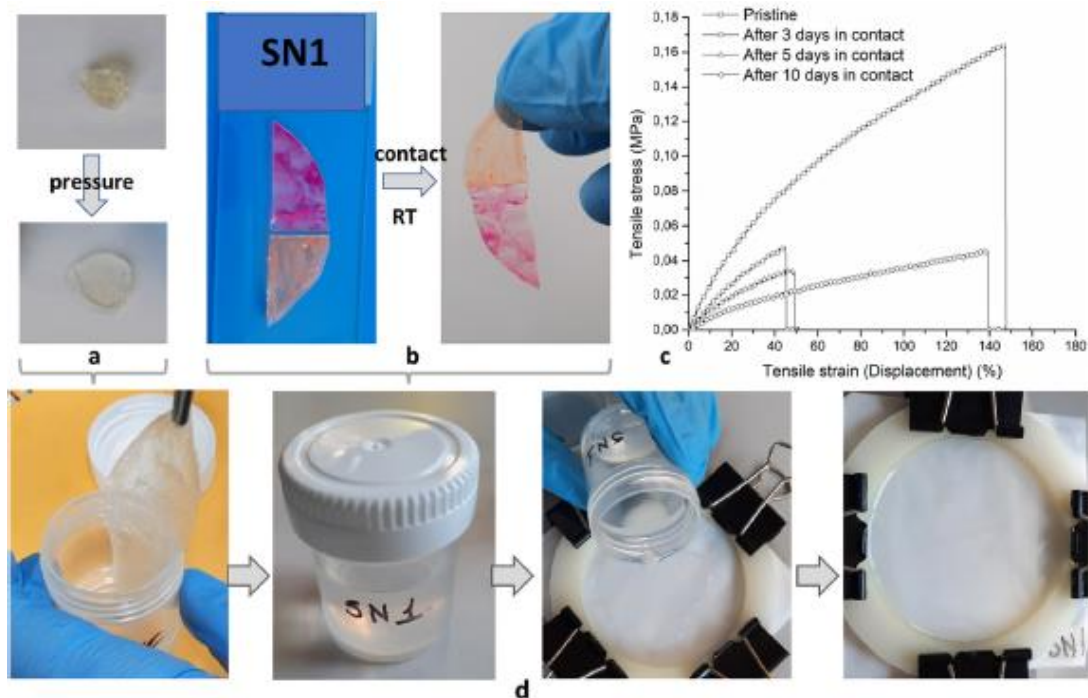


Figure 5.47. Visual evidence of the self-repair capacity of the prepared supramolecular networks, exemplified for SN1 network: by pressing the grouped pieces (a); by simply contacting the pieces for a while at room temperature (b), and stress-strain curves in different stages of the self-healing process of the SN1 network at room temperature (c). Solvoplastic behavior of SN1 (d).

V.3.6.1. Study of the reversibility of supramolecular interactions by FTIR spectroscopy

Carbamate groups were formed by exposing the samples to air during drying at room temperature. Their presence is confirmed by the bands at $1740\text{-}1680\text{ cm}^{-1}$ assigned to amide I groups in carbamate, while ionic carboxylate groups are identified by asymmetric and symmetric vibrations at 1570 cm^{-1} and 1338 cm^{-1} . The position of these bands is similar to that in the IR spectrum of the sodium salt of the **PDMS-COOH** precursor. Spectra recorded over the time of the cooling process from 120 to $80\text{ }^{\circ}\text{C}$ showed changes in the position and intensity of the band at 1710 cm^{-1} specific to free carboxyl groups but also shifts at lower wavenumbers of the bands specific to the N-H bond deformation vibrations, similar to the original spectra of the samples, demonstrating hydrogen bond refolding. In the spectra recorded upon cooling to $40\text{ }^{\circ}\text{C}$, absorption maxima were observed at $1730\text{-}1720\text{ cm}^{-1}$ which are characteristic of amide I bonds in carbamate groups. In the formation of carbamate groups, hydrogen bonds, hydrophobic environment and humid atmosphere play an important role. The mechanism consists of nucleophilic attack of CO_2 by amines leading to R-

$\text{NH}_2^+\text{COO}^-$, assisted/catalysed by amine, water and OH groups, which can subsequently form either ammonium carbamate or carbamic acid, depending on the inter/intramolecular proton transfer [299].

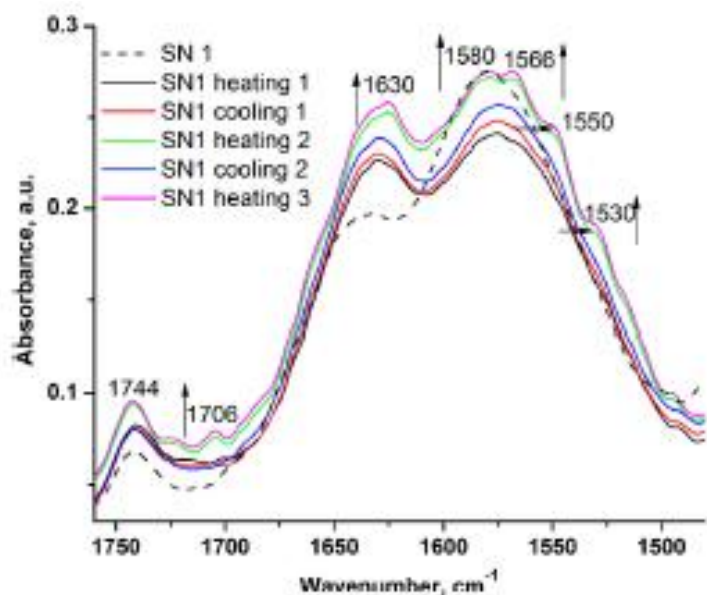


Figure 5.52. IR absorbance spectra of SN1 network before and after heating/cooling processes

The co-existence of intermolecular hydrogen bonding and ionic interactions has also been demonstrated by repeated heating/cooling processes of the SN1 network prepared in an inert atmosphere in a drybox. IR spectra revealed the appearance upon heating of the band at 1706 cm^{-1} attributed to free COOH groups and the shift to lower wavenumbers of the bands at 1580 , 1566 , 1550 and 1530 cm^{-1} attributed to N-H bond deformation vibrations and C-O and C-N bond specific stretching vibrations. On cooling, the bands attributed to free COOH groups disappeared, suggesting hydrogen bond reforming between COOH and NH_2 (**Figure 5.52.**).

V.3.6.2. Study of the reversibility of supramolecular interactions by dielectric spectroscopy

The dynamics of supramolecular interactions have also been revealed by temperature-dependent dielectric spectroscopy studies. As the temperature increases, a number of processes occur in the lattice that influence its dielectric permittivity: hydrogen bond breaking, ionic bond dissociation (as evidenced by IR studies with temperature) and increased mobility of segments that facilitate dipole orientation [295]. While hydrogen bond suppression decreases the dielectric permittivity, ionic pair dissociation leads to increased dielectric permittivity with increasing temperature. The mobility of the siloxane chain is affected by the degree of cross-linking through established intermolecular interactions, decreasing with increasing intermolecular interactions, but is insignificantly affected by temperature. In contrast, the organic segments through which polar groups are attached to the siloxane chain can be affected by temperature. As a result, there are several grid parameters that change with

increasing temperature and can influence the dielectric permittivity differently, leading to a more complex shape of its variation, as can be seen in **Figure 5.53**.

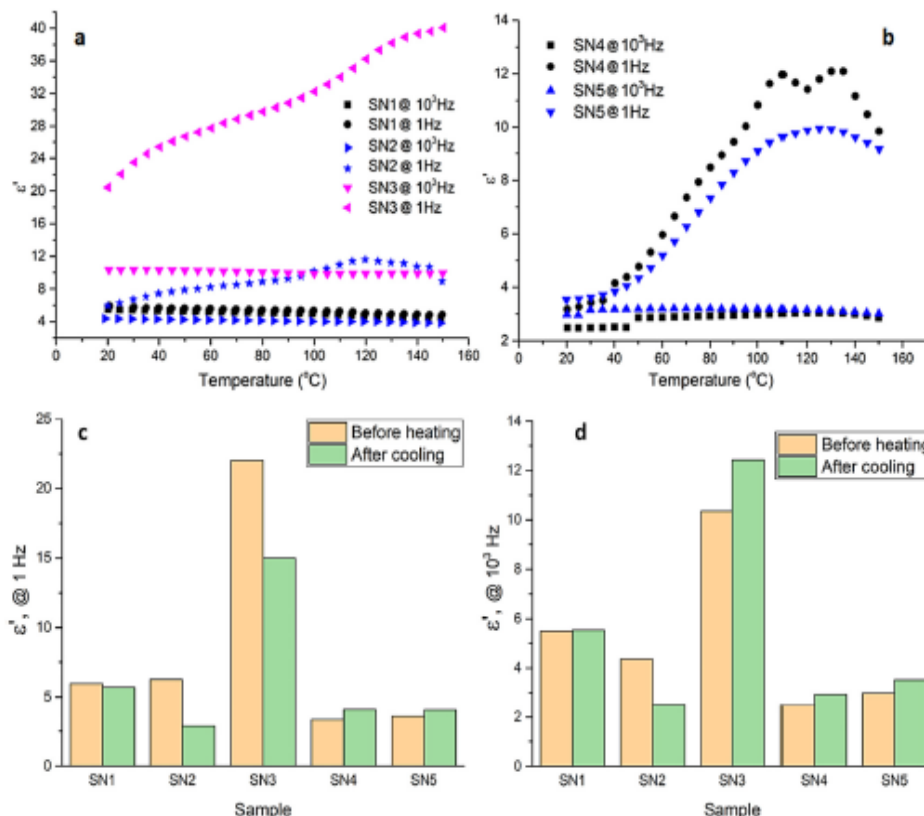


Figure 5.53. Variation of dielectric permittivity, ϵ' , with temperature at 1 Hz and 103 Hz for series SN1-SN3 (a) and SN4-SN5 (b); Changing the dielectric permittivity, ϵ' , value at room temperature, before and after heating to 150 °C to 1 Hz (c) and 103 Hz (d)

V.4.3.1. Swelling capacity of supramolecular networks

Swelling experiments were performed by immersing samples of well-determined mass and volume in water, buffer solutions of pH 2.6, 5.0 and 7.4 and chloroform at room temperature.

Table 5.23. Swelling capacity of materials immersed in different media

Sample	Water	PBS			Chloroform
		pH 2.6	pH 5.0	pH 7.4	
SN1	71%	77%	18%	3%	-
SN2	86%	84%	31%	72%	80%
SN3	37%	163%	20%	26%	125%
SN4	9%	12%	14%	12%	-
SN5	52%	12%	26%	20%	36%
	SN2>SN1>SN5> SN3>SN4	SN3>SN2>SN1> SN4=SN5	SN2>SN5>SN3> SN1>SN4	SN2>SN3>SN5> SN4>SN1	SN1, SN4: dezinintegration; SN3>SN2> SN5

Although the profile of the swelling curves is very different for the five samples, after 72 h they all reached the maximum level. Regardless of the immersion medium, **SN4** and **SN5** grids generally had lower swelling capacity than the **SN1-SN3** series due to the higher degree of cross-linking. The **SN5** network swelled the most in water, about 50%, while in buffer solutions up to about 20%. In the **SN1-SN3** series, in pH 2.6 buffer solution, the swelling capacity increases with the content of protonated carboxyl and amino groups, while at pH 5 and 7.4, the **SN2** sample, having an equal ratio of amino and carboxyl groups, swells the most and **SN1** the least. A higher concentration of protonated groups in **SN1** may promote some electrostatic interactions with the citrate and phosphate medium reducing the swelling ratio [306]. Sample **SN2** also swells most strongly in water. The presence of hydrophilic ammonium carboxylate groups enhanced the permeation of water into the lattice increasing the swelling ratio, while the lower swelling in water of sample **SN3** is due to the higher content of carboxylic groups involved in stronger hydrogen ionic bonds, decreasing the permeation in water.

CHAPTER VI - DUAL SILICONE COVALENT / SUPRAMOLECULAR POROUS NETWORKS

VI.2. Obtaining porous networks

Polydimethyl(3-aminopropyl)methylsiloxane- α,ω -diols, **PDMS-NH₂-1,2,3**, with different contents of amino groups (6.4 mol%, 9.4 mol% and 100 mol%, respectively) were prepared by a procedure involving successive hydrolysis/polymerization/ring-opening equilibration starting directly from octamethylcyclotetrasiloxane (D₄) and 3-aminopropyl(diethoxy)methylsilane in different molar ratios, in the presence of KOH and DMSO [345]. These were used as precursors to obtain covalently cross-linked silicon (PN) networks by acetic acid-catalyzed condensation of OH-terminal groups with TEOS in the presence of ammonium bicarbonate as a chemical expanding agent (CBA).

Decomposition of CBA occurs by heating the mixture in acidic medium (*Scheme 6.20*).

VI.3.2. Reversibility of carbamate bonds

The lability of carbamate groups was investigated on sample **PN9**, from the polysiloxane with the highest content of NH_2 groups. ATR-IR spectroscopy was used to study the behavior of the sample in heating/cooling processes. IR spectra were recorded first at room temperature and then by increasing the temperature to $120\text{ }^\circ\text{C}$. The sample was held at this temperature for 20 minutes, with spectra measured every 5 minutes. After the heating process, the sample was left at room temperature for cooling and the spectra were measured every 5 min during the cooling process. IR spectra in the spectral range $1800\text{-}1270\text{ cm}^{-1}$ are presented in **Figure 6.64**. The absorption of CO_2 in sample **PN9** was confirmed by the presence of carbamate groups formed during the cross-linking process at room temperature. CO_2 uptake by amino-functionalized compounds has been shown to be influenced by ambient temperature and humidity, with lower temperature favoring high CO_2 uptake, while higher water content will favor the formation of ammonium bicarbonate [350].

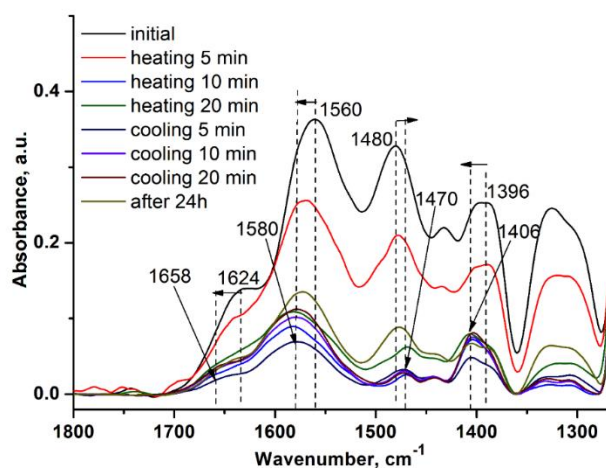


Figure 6.64. ATR-IR spectra of **PN9** sample during heating/cooling processes highlighting the carbamate degradation and regeneration of the primary amino groups

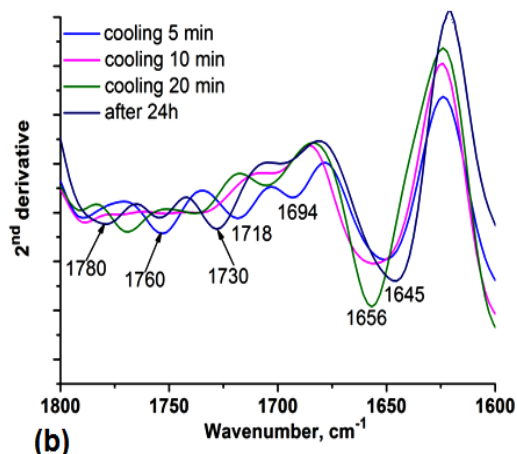
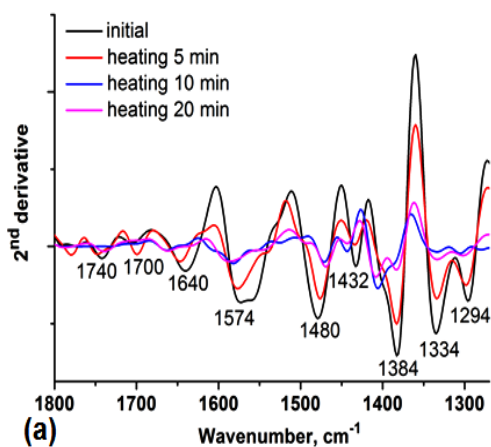


Figure 6.65. The 2nd derivative of the IR spectrum of **PN9** during the heating (a) and cooling (b) processes within $1800\text{-}1270\text{ cm}^{-1}$ spectral range

To regenerate the NH_2 groups in sample **PN9** carbonated during crosslinking, the sample was heated to $120\text{ }^\circ\text{C}$ to break the C-N bonds specific to carbamate groups. By heating, the sample, the absorption maxima at $1700\text{-}1740\text{ cm}^{-1}$ assigned to the carbamate groups diminished until disappearance supporting the degradation of the carbamate groups. At the same time, the bands at 1624 cm^{-1} and 1560 cm^{-1} (assigned to NH_3^+ asymmetric and symmetric deformation vibrations) and 1396 cm^{-1} (assigned to C-N stretches) are redshifted by $10\text{-}30\text{ cm}^{-1}$, proving the regeneration of the primary amino groups (**Figure 6.65.a**). On cooling the sample at room temperature one can observe the appearance of the characteristic absorption maxima for carbamate group at $1780\text{-}1694\text{ cm}^{-1}$. (**Figure 6.65.b**).

VI.3.3. Morphology of porous networks

The **PN1-PN6** networks, based on polysiloxane precursors with a relatively low degree of functionalization (6.4 and 9.8 mol% amino groups), are visibly porous, with very large pores, on the order of hundreds of micrometers, generated by the gases of decomposition of ammonium bicarbonate. A high amount of blowing agent led, in the case of **PN1-PN6**, to a noticeable decrease in the network density, the effect being attributed to the increased gas yield and the number of bubbles generated. However, an exact dependence of the network density on the foaming agent is relatively difficult to predict because, at a higher amount of gas generated in the network, some bubbles may break, so the network density may increase in this case [344].

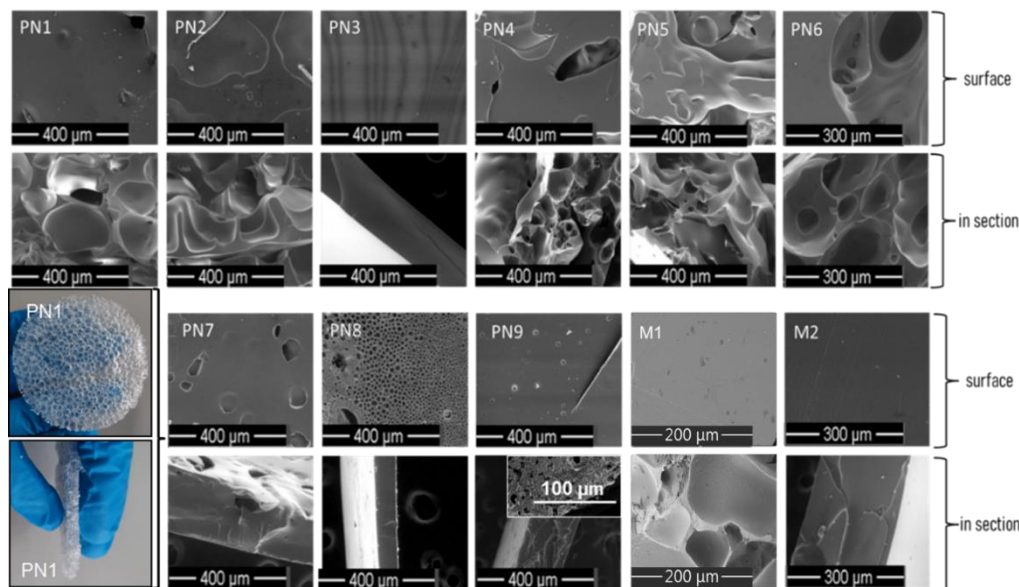


Figure 6.66. Photo images of the **PN1** sample (bottom left corner) and SEM images on surface and in section of the porous networks

In these cases, the pore nucleation density increases and the development of gas bubbles occurs. The instability induced by gas diffusion in the already generated bubbles causes them to

rapidly grow to a critical size, at which they burst and collapse. This explains the reduction in the proportion of large pores and the densification of the material [344]. Because of the wide polydispersity of the pore size, the samples were not suitable for recording nitrogen sorption isotherms, so establishing a precise correlation between the amount of porogenic agent and porosity was not possible by this technique.

VI.3.6. Analysis of dielectric properties

The dielectric properties of the porous silicone networks with different contents of pendant aminopropyl groups were studied in comparison with those of the two reference materials based on polydimethylsiloxane, the dielectric spectra being shown in **Figure 6.68**. Reference samples **M1** and **M2** have dielectric permittivity values of approximately $\epsilon' = 5$ and 4 at 104 Hz, respectively, which remain constant over the entire frequency range. Dielectric losses follow the same trend. Although some samples (**PN4** and **PN5**, for example) show higher dielectric permittivity values in the range 0.1–104 Hz, at higher frequencies, all samples show values in the range 5–6, similar to interpenetrated ionic/silicon networks, where higher ionic network concentration does not necessarily induce higher permittivity at higher frequencies [354]. Dielectric loss values are relatively high (e.g. 103 for **PN4** and **PN5**), and continuously decrease to below 1 as the frequency increases (**Figure 6.68.b**).

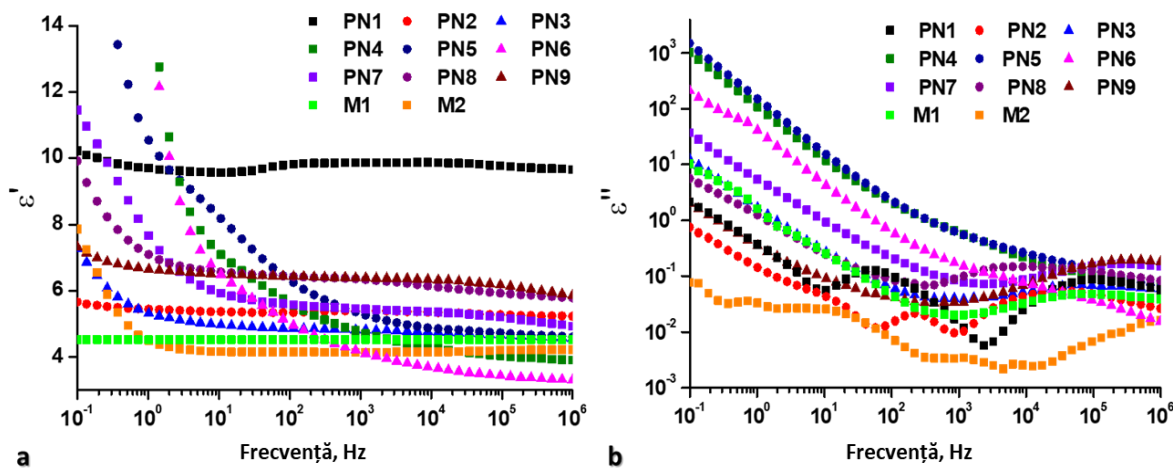


Figure 6.68. Dielectric permittivity (a) and dielectric loss (b) for samples **PN1-PN9** and **M1-M2** as references

VI.3.8. Relative capacitance modification

Several porous networks (**M1**, **PN1**, **PN5** and **PN9**) were selected and tested for their suitability as pressure sensors. The samples were analyzed after reaching mechanical stability, as

can be seen in **Figure 6.71**. Thus, compression (at 30%, with a speed of 10 mm/min) and associated capacitance changes were recorded cyclically (10 cycles). It was observed that the cyclic change of the capacitance, depending on the applied compression, shows repeatability, good response time and linearity, $R^2 > 0.92$ for the pressure domains below 30 kPa, without drift overshoots being recorded [355]. An exception is sample **M1**, for which a very noisy capacitance was recorded.

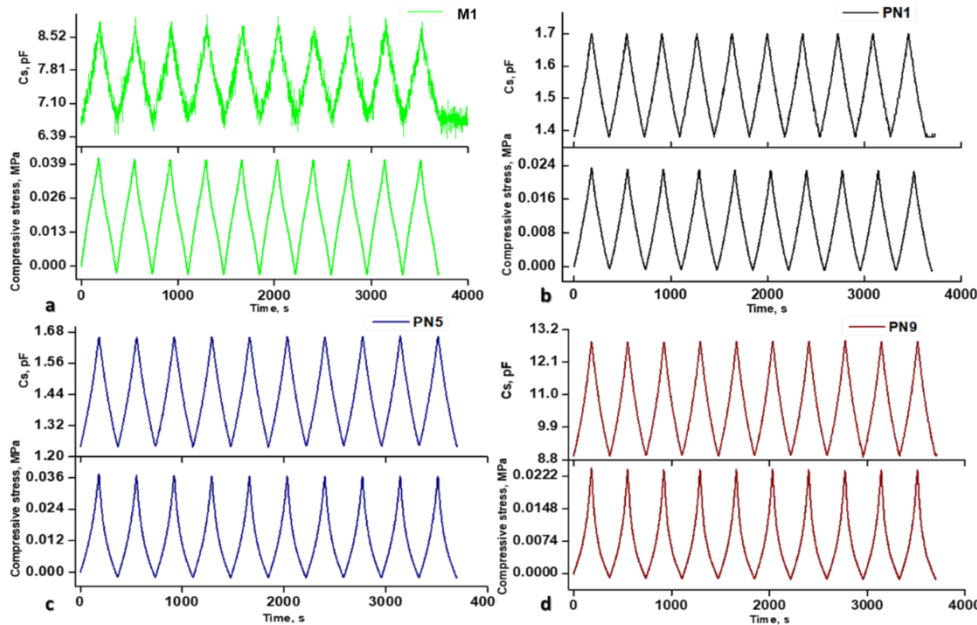


Figure 6.71. Correlation between the capacitance change and applied compressive stress for reference sample **M1** and **PN1**, **PN5** and **PN9** porous samples

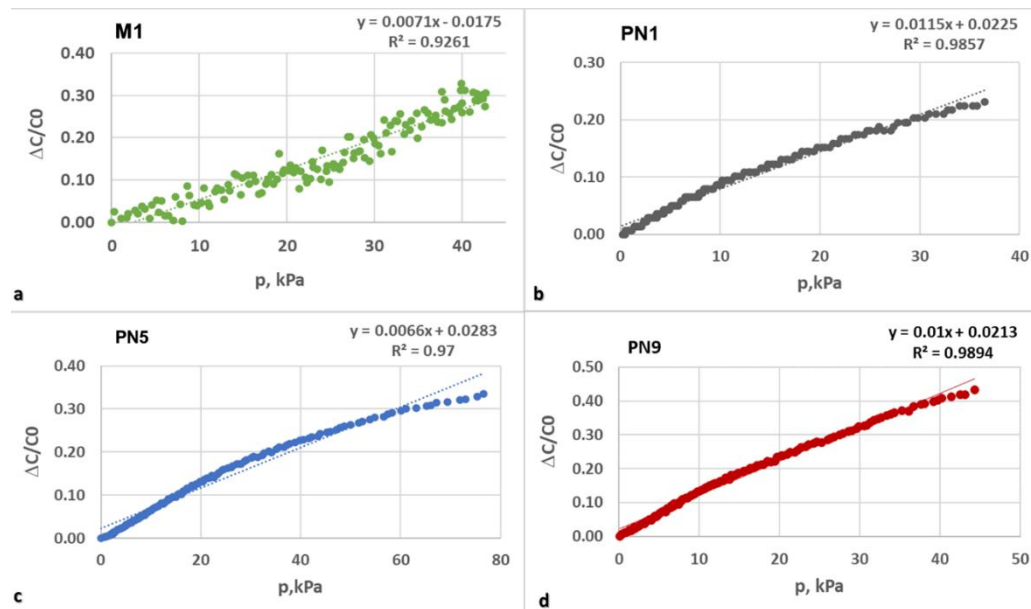


Figure 6.73. Pressure sensing performance of polar porous networks (**PN1**, **PN5** and **PN9**) compared to a non-polar one (**M1**)

It can be seen that, at a lower pressure range (< 10 kPa), sample **M1** has unstable capacitance variations and low sensitivity, unable to be used as a sensor in this pressure range, **PN1**, **PN5** and **PN9**, showed a stable capacitance variation, with a maximum $\Delta C/C_0$ around 0.09,

0.065, and 0.13, resp., and with very good linearities ($R^2 > 0.92$) and moderate sensitivities ($\sim 0.01 \text{ kPa}^{-1}$). An exception is sample **PN5**, which has a high dielectric loss (**Figure 6.68.b**). The same behavior was observed at a higher pressure range (0 – 30 kPa), with low $\Delta C/C_0$ (< 0.05) at a low pressure range ($< 4 \text{ kPa}$), indicating that the samples could be successfully used as sensors for monitoring changes in heart rate or respiration during/after exercise [356]. Increasing the applied pressure leads to a higher value for $\Delta C/C_0$ (**Figure 6.73.**), expanding the application possibilities to devices such as robotic hands capable of grasping light objects..

CHAPTER VII - GENERAL CONCLUSIONS

Five types of silicone derivatives consisting of novel compounds (silatranes) and materials (covalent, supramolecular and covalent/supramolecular porous silicas and silicone networks) were prepared, from the perspective of evaluating their suitability for biomedical applications. In almost all cases, to obtain the desired products, the synthesis of suitable precursors was necessary, namely, 3-aminopropylsilatran, polysiloxanes functionalized on the ends or on the chain with OH, vinyl, Si-H or SH groups, copolymers dimethylmethyl(3-aminopropyl) or dimethylmethyl(carboxyethyl-thiopropyl)siloxanes and octakis(2-carboxymethyl-thioethyl)silsesquioxane (T8-COOH), which were isolated, purified and structurally characterized. The products obtained on their basis by derivatization or cross-linking through different mechanisms have been characterized, in general, from the point of view of structure, morphology, thermal, surface, mechanical, dielectric behavior as well as properties of biological interest (biocompatibility, cytotoxicity, activity antifungal and antibacterial, bio/mucoadhesivity, as appropriate).

- Chemical modification of 3-aminopropyl silatran with 5-nitrosalicylaldehyde led to a new Schiff base derivative with moderate protein binding capacity. The nitro derivative showed specific interactions with human and bovine albumin, including a 1:1 interaction with BSA, and showed M^{PRO} protein binding affinity comparable to the antiviral drugs chloroquine and hydroxychloroquine. It also demonstrated increased mucoadhesion and superior cytotoxicity on MCF7 cells compared to HepG2 cells. These results suggest that this derivative could be a promising antitumor therapeutic agent, requiring further investigation to elucidate its cytotoxic mechanism in *in vivo* situations.

- The study of mesoporous silica (MS) particles modified in-situ with different groups shows that those functionalized with amino and hydroxyl groups are effective antimicrobial and

mucoadhesive agents. The antimicrobial properties, comparable to those of the antibiotic Kanamycin and the antifungal Caspofungin, together with the improved mucoadhesion, suggest a potential in the development of drug carriers based on them. Doxorubicin (DOX) release studies revealed varying efficiency depending on the degree of functionalization and the pH of the medium. The best results were recorded for amino-functionalized MS at lower pH and for that with hydroxyl groups at neutral pH. Cytotoxicity was seen at concentrations greater than 30 $\mu\text{g}/\text{mL}$ on normal cells. The increased selectivity on MCF-7 cells indicates the potential of these particles for anticancer therapy.

- Covalently cross-linked silicone films, which differ in density and cross-linking pattern, exhibit different surface morphologies and physical (contact angle) or chemical (with the release of small molecular compounds as a result of hydrolysis) interactions with different media. Spectroscopic analysis indicated the presence of secondary products, and surface analysis revealed nanometric roughness. The hydrophobic properties of the silicone films were highlighted by relatively high values of the contact angle with water and PBS solutions indicating their hydrophobic character. Topography, surface chemistry, but also physical or chemical interactions between surfaces have been shown to play an essential role in bioadhesion. Blood compatibility was assessed by interfacial tension with blood, with results suggesting a reduced risk of thrombosis in the short term. Bioadhesive and mucoadhesive properties have been associated with the presence of residual unreacted functional groups, which favor cell adhesion and antimicrobial activity. In general, based on the highlighted properties, these films are recommended for short-term medical applications such as sutures or covering materials, while the R4-3 film, with an increased mucoadhesion, can be considered as a potential support for the local release of bioactive compounds.

- Supramolecular silicone networks were prepared by self-assembling dimethylsiloxane polymers, having low content of amino (PDMS-NH₂) and carboxyl groups (PDMS-COOH) or with a polycarboxylated octasilsesquioxane (POSS-COOH). Free-standing films obtained by supramolecular self-assembly exhibit self-repair and recycling capability. IR studies revealed the dynamics of supramolecular (hydrogen) bonds, confirming thermoplasticity. The materials are also solvoplastic, they can be reprocessed by dissolving in a minimal amount of THF which, according to data from the literature, does not have a major negative impact on health or the environment. The thermal stability of the materials was confirmed by thermogravimetric analysis. The high dielectric permittivity and low Young's modulus values make them suitable as electroactive dielectric elastomers. The tests carried out, from the perspective of their use as biomaterials, showed

compatibility with fibroblast cells and antimicrobial capacity for some samples. Evaluation of swelling in simulated biological environments revealed mucoadhesive behavior, crucial for the design of drug delivery systems. The content of carboxyl groups strongly influences the detachment force from biomucous, and networks with a reduced $-\text{COOH}/-\text{NH}_2$ ratio showed the highest recycling capacity, thus being of great interest from the perspective of green chemistry.

- A series of nine porous networks based on polysiloxanes functionalized with aminopropyl groups and two cross-linked reference samples were successfully developed, which were analyzed from a structural and some properties point of view. The obtained materials presented reasonable mechanical, thermal and dielectric properties, being characterized by an increased antimicrobial activity due to the presence of amino and carbamate groups. The crosslinking process was a dual one involving covalent crosslinking with TEOS in the absence of metal catalysts and supramolecular through dynamic carbamate bridges in the presence of CO_2 , generated *in situ*, which led to porous morphologies. The presence of polar groups has the effect of increasing the dielectric permittivity which changes depending on the applied pressure. Thus, these porous materials have potential for use in pressure sensors and in applications that require biocompatibility and stability under variable conditions.

For all the compounds and materials obtained from this thesis, similar protocols of structural characterization as well as material characteristics (morphology, mechanical behavior, thermal, dielectric, etc.) were applied, so that materials with the best properties, from the perspective of use as biomaterials.

Thus, in the case of the SIL M and SIL-BS silatranic compounds, both compounds were noted for their increased adhesion, which may favor an optimized therapeutic effect by increasing the permeability of the drug and the contact time at the tumor sites. Additional benefits of these compounds have been demonstrated by their antimicrobial activity against several species of bacteria and fungi. Molecular docking calculations have also demonstrated their potential in the development of new drugs for combination therapy.

Due to their structural, morphological, and behavioral characteristics (e.g., tunable volume and pore size, functionalization possibilities, excellent biocompatibility, controlled stability and biodegradation, ability to protect the encapsulated drug against premature release and unwanted degradation), functionalized mesoporous silica particles M1s have the potential to be promising

diagnostic and delivery platforms, with a key role in the development of next-generation formulations.

The results of covalent network analyzes indicate that, regardless of the crosslinking pattern, the films are hydrophobic, hydrolytically stable and biocompatible with lower bio-/mucoadhesion values, recommending them in biomedical applications such as sutures, of which noting the R4 series.

The supramolecular nature of networks of this type obtained, without the need for catalysts, was highlighted and exploited through self-repair capacity, solvoplasticity in solvents with different polarities and environments that mimic biological fluids. All this indicates the sustainability of these materials.

In the case of porous networks, the presence of polar groups led to an increase in the dielectric permittivity of the materials, this fact being most evident in the case of the porous material PN9, with the most functional groups. This material also presented the best performance in testing as a capacitive pressure sensor.

Originality aspects

Through a complex and innovative approach, the thesis contributes to the field of biomaterials research, the main elements of originality being:

- Development of new compounds and materials with biomedical potential through complex synthetic approaches, proprietary or adapted. The thesis covers five types of silicone derivatives, each with a specific purpose and distinct properties.

- Synthesis of suitable precursors, such as 3-aminopropylsilatran, polysiloxanes functionalized with amino and carboxy groups, and octakis(2-carboxymethylthioethyl)silsesquioxane (T8-COOH).

- Holistic approach in selecting and evaluating materials for biomedical applications. The obtained materials were characterized in terms of structural, morphological, thermal, surface, mechanical, dielectric and biological properties.

- Characterization of silatran compounds included interactions with proteins, such as human and bovine albumin, and antimicrobial activity against bacteria and fungi. These aspects suggest the potential of these materials in the development of multifunctional therapeutic agents.

•Functionalized mesoporous silica particles were evaluated, not only for their ability to transport doxorubicin, but also for their antimicrobial activity and mucoadhesion. This integrated approach adds an additional dimension to materials research for biomedical applications.

• Supramolecular networks showed self-repair and recyclability properties, highlighting a sustainable and innovative aspect in the development of materials, including for the biomedical field.

• Porous materials have been designed to function as biomaterials including as pressure sensors, with potential for use in pulse or respiration monitoring in exercise.

•Characterization of the silicone films included evaluation of blood compatibility, indicating possible use in short-term medical applications such as sutures or coating materials.

SELECTIVE BIBLIOGRAPHY

1. J. Curtis, A. Colas, Medical Applications of Silicones. Biomaterials Science, p.1106–1116. doi:10.1016/b978-0-08-087780-8.00107.
2. M. Zare, E. R. Ghomi, P. D. Venkatraman, S. Ramakrishna, J Appl Polym Sci 2021, e50969. <https://doi.org/10.1002/app.50969>.
3. J. A. González Calderón, J. D. Contreras López, E. Pérez, J. Vallejo Montesinos, Polysiloxanes as polymer matrices in biomedical engineering: their interesting properties as the reason for the use in medical sciences. Polymer Bulletin. 2019, doi:10.1007/s00289-019-02869-x
4. K. Mojsiewicz-Pieńkowska, Safety and Toxicity Aspects of Polysiloxanes (Silicones) Applications, Concise Encyclopedia of High Performance Silicones, Scrivener Publishing LLC, 2014, p. 243–252
5. G. Schalau, H. Aliyar, Recent Developments on Silicones in Topical and Transdermal Drug Delivery, Dow Corning Corporation, Healthcare Industry, Pharmaceuticals, Midland, Michigan 48686, USA
6. M.G. Voronkov, Chapter 27. Silicon in biology and medicine, Annu. Reports Med. Chem, Elsevier (1975), pp. 265-273. [https://doi.org/10.1016/S0065-7743\(08\)61015-5](https://doi.org/10.1016/S0065-7743(08)61015-5)
7. J. J. Petkowski, W. Bains, S. Seager, On the Potential of Silicon as a Building Block for Life. Life (Basel, Switzerland), 10(6), 2020, 84. <https://doi.org/10.3390/life10060084>
8. A. Mashak, A. Rahimi, Silicone Polymers in Controlled Drug Delivery Systems: A Review, Iranian Polymer Journal, 2009 18(4), 279-295.
9. B. Reilly, Silicones as a Material of Choice for Drug Delivery Applications. 2004

10. V.-C. Niculescu, Mesoporous Silica Nanoparticles for Bio-Applications. *Front. Mater.* (2020) 7:36. doi: 10.3389/fmats.2020.00036.
11. K. Zalewski, Z. Chyłek, W. A. Trzciński, A Review of Polysiloxanes in Terms of Their Application in Explosives. *Polymers*, 13(7), 2021, 1080. <https://doi.org/10.3390/polym13071080>
131. A.-M.-C. Dumitriu, M. Cazacu, S. Shova, C. Turta, B.C. Simionescu, Synthesis and structural characterization of 1-(3-aminopropyl)silatrane and some new derivatives. *Polyhedron* 2012, 33, 119–126
132. A. Bargan, M.F.Zaltariov, A. Vlad, A.-M.-C. Dumitriu, A. Soroceanu, A.-M. Macsim, M. Dascalu, C.D. Varganici, M. Cazacu, S. Shova, Keto-enol tautomerism in new silatranes Schiff bases tailed with different substituted salicylaldehyde. *Arab. J. Chem.* 2020, 13, 3100–3111
139. Herzfeld, R.; Nagy, P. Studies of the Solvent Effect Observed in the Absorption Spectra of Certain Types of Schiff Bases. *Curr. Org. Chem.* 2001, 5, 373–394
141. Khalaji, A.D.; Foroghnia, A.; Khalilzadeh, M.A.; Fejfarova, K.; Dušek, M. 2-(3,4-Dimethoxyphenyl)-1H-benzimidazole. *Acta Cryst.* 2011, 67, o3255
149. Nepali, K.; Lee, H.-Y.; Liou, J.-P. Nitro Group Containing Drugs. *J. Med. Chem.* 2019, 62, 2851–2893
158. Trott, O.; Olson, A.J. AutoDock Vina: Improving the speed and accuracy of docking with a new scoring function, efficient optimization, and multithreading. *J. Comput. Chem.* 2010, 31, 455–461
159. Krieger, E.; Vriend, G. YASARA View—Molecular graphics for all devices—From smart phones to workstations. *Bioinformatics* 2014, 30, 2981–2982
160. Krieger, E.; Koraimann, G.; Vriend, G. Increasing the precision of comparative models with YASARA NOVA—A selfparameterizing force field. *Proteins* 2002, 47, 393–402
170. Thurakkal, L.; Singh, S.; Roy, R.; Kar, P.; Sadhukhan, S.; Porel, M. An in-silico study on selected organosulfur compounds as potential drugs for SARS-CoV-2 infection via binding multiple drug targets. *Chem. Phys. Lett.* 2021, 763, 138193
196. Huh, S.; Wiench, J.W.; Yoo, J.-C.; Pruski, M.; Lin, V.S.-Y. Organic Functionalization and Morphology Control of Mesoporous Silicas via a Co-Condensation Synthesis Method. *Chem. Mater.* 2003, 15, 4247–4256
197. Cordeiro, R.; Carvalho, A.; Durães, L.; Faneca, H. Triantennary GalNAc-Functionalized Multi-Responsive Mesoporous Silica Nanoparticles for Drug Delivery Targeted at Asialoglycoprotein Receptor. *Int. J. Mol. Sci.* 2022, 23, 6243
210. Barbé, C., Bartlett, J., Kong, L., Finnie, K., Lin, H. Q., Larkin, M., ... Calleja, G. (2004). Silica Particles: A Novel Drug-Delivery System. *Advanced Materials*, 16(21), 1959–1966. doi:10.1002/adma.200400771

217. M. Pishnamazi, H. Hafizi, M. Pishnamazi, A. Marjani, S. Shirazian, G.M. Walker, Controlled release evaluation of paracetamol loaded amine functionalized mesoporous silica KCC1 compared to microcrystalline cellulose based tablets, *Sci. Rep.* 11(2021) 535
226. D. Preisig, R. Roth, S. Tognola, F.J.O. Varum, R. Bravo, Y. Cetinkaya, J. Huwyler, M. Puchkov, Mucoadhesive microparticles for local treatment of gastrointestinal diseases, *Eur. J. Pharm. Biopharm.* 105 (2016)156-165
227. R. Huang, Y.-W. Shen, Y.-Y. Guan, Y.-X. Jiang, Y. Wu, K. Rahman, L.-J. Zhang, H.-J. Liu, X. Luan, Mesoporous silica nanoparticles: facile surface functionalization and versatile biomedical applications in oncology, *Acta Biomater.* 116 (2020) 1-15
284. W. Zang, X. Liu, J. Li, Y. Jiang, B. Yu, H. Zou, N. Ning, T. Ming, L. Zhang, Conductive, self-healing and recyclable electrodes for dielectric elastomer generator with high energy density, *Chem. Eng. J.* 429 (2022), 132258, <https://doi.org/10.1016/j.cej.2021.132258>
286. J. Mo, X. Chen, Y. Fu, R. Li, Y. Lin, A. Zhang, A solvent-free, transparent, selfhealing polysiloxanes elastomer based on unsaturated carboxyl-amino ionic hydrogen bonds, *Polymer* 228 (2021), 123903, <https://doi.org/10.1016/j.polymer.2021.123903>
287. G. Socrates, *Infrared and Raman Characteristic Group Frequencies*, 3rd edition, John Wiley and Sons, Chichester, England, 2004, pp. 126–256
293. F. Pizzitutti, F. Bruni, Electrode and interfacial polarization in broadband dielectric spectroscopy measurements, *Rev. Sci. Instrum.* 72 (2001) 2502
294. M. Samet, V. Levchenko, G. Boiteux, G. Seytre, A. Kallel, A. Serghei, Electrode polarization vs. Maxwell-Wagner-Sillars interfacial polarization in dielectric spectra of materials: Characteristic frequencies and scaling laws, *J. Chem. Phys.* 142 (19) (2015), 194703, <https://doi.org/10.1063/1.4919877>
295. J. Ortiz de Urbina, G. Sesé, Influence of hydrogen bonds and temperature on dielectric properties, *Phys. Rev. E* 94 (1) (2016), <https://doi.org/10.1103/physreve.94.012605>
296. S. Jana, S. Garain, S. Sen, D. Mandal, The influence of hydrogen bonding on the dielectric constant and the piezoelectric energy harvesting performance of hydrated metal salt mediated PVDF films, *Phys. Chem. Chem. Phys.* 17 (26) (2015) 17429–17436, <https://doi.org/10.1039/c5cp01820j>
297. T. Song, B. Jiang, Y. Li, Z. Ji, H. Zhou, D. Jiang, I. Seok, V. Murugadoss, N. Wen, H. Colorado, Self-healing materials: A review of recent developments, *ES Mater. Manuf.* 14 (2021) 1–19, <https://doi.org/10.30919/esmm5f465>
298. M.T. Cook, V.V. Khutoryanskiy, Mucoadhesion and mucosa-mimetic materials—A mini-review, *Int. J. Pharm.* 495 (2) (2015) 991–998, <https://doi.org/10.1016/j.ijpharm.2015.09.064>
299. R.B. Said, J.M. Kolle, K. Essalah, B. Tangour, A. Sayari, A unified approach to CO₂- amine reaction mechanisms, *ACS Omega* 5 (40) (2020) 26125–26133, <https://doi.org/10.1021/acsomega.0c03727>

306. A. Słoniewska, M. Kasztelan, S. Berbeć, B. Palys, Influence of buffer solution on structure and electrochemical properties of poly(3,4-ethylenedioxythiophene)/poly(styrenesulfonate) hydrogels, *Synth. Met.* 263 (2020), 116363, <https://doi.org/10.1016/j.synthmet.2020.11636>
345. B.-I. Ciubotaru, M. Dascalu, M.-F. Zaltariov, A.-M. Macsim, M. Damoc, A. Bele, C. Tugui, C.-D. Varganici, M. Cazacu, 2022. Catalyst-free crosslinked sustainable functional silicones by supramolecular interactions. *React. Funct. Polym.* 105419. <https://doi.org/10.1016/j.reactfunctpolym.2022.105419>
350. L. B. Hamdy, C. Goel, J. A. Rudd, A. R. Barron, E. Andreoli, The application of amine-based materials for carbon capture and utilisation: an overarching view, *Mater. Adv.* 2 (2021) 5843-5880. <https://doi.org/10.1039/D1MA00360G>.
354. P. J. Flory, *Principles of Polymer Chemistry*, Cornell University Press, Ithaca, New York, 1953.
355. R. S. Maxwell, B. Balazs, Residual dipolar coupling for the assessment of crosslink density changes in γ -irradiated silica-PDMS composite materials, *J. Chem. Phys.* 116 (2002) 10492-10502. <https://doi.org/10.1063/1.1477184>.
356. D. Sahu, R. K. Sahu, K. Patra, Effects of crosslink density on the behavior of VHB 4910 dielectric elastomer, *J. Macromol. Sci. A* 56 (2019) 821–829. <https://doi.org/10.1080/10601325.2019.1610329>.

SCIENTIFIC ACTIVITY

ISI articles published within the thesis:

1. **B.-I. Ciubotaru**, M.-F. Zaltariov, M. Dascalu, A. Bele, A. Bargan, M. Cazacu. Amino-functionalized silicones processed as porous dual covalent/supramolecular networks for pressure sensing. *Reactive and Functional Polymers* (2024) 105792. (FI = 5.1), (Q1).
2. M.-F. Zaltariov, **B.-I. Ciubotaru**, A. Ghilan, D. Peptanariu, M. Ignat, M. Iacob, N. Vornicu, M. Cazacu. Mucoadhesive Mesoporous Silica Particles as Versatile Carriers for Doxorubicin Delivery in Cancer Therapy. *International Journal of Molecular Sciences* (2023) 24(19), p.14687. (FI = 5.6), (Q2).
3. M.-F. Zaltariov, M. Turtoi, D. Peptanariu, A.-M. Macsim, L. Clima, C. Cojocar, N. Vornicu, **B.-I. Ciubotaru**, A. Bargan, M. Calin, M. Cazacu, Chemical Attachment of 5-Nitrosalicylaldimine Motif to Silatrane Resulting in an Organic–Inorganic Structure with High Medicinal Significance, *Pharmaceutics* (2022) 14, 2838 <https://doi.org/10.3390/pharmaceutics14122838> (FI = 5.4), (Q2).
4. **B.-I. Ciubotaru**, M. Dascalu, M.-F. Zaltariov, A.-M. Macsim, M. Damoc, A. Bele, C. Tugui, C.-D. Varganici, M. Cazacu, Catalyst-free crosslinked sustainable functional silicones by supramolecular interactions, *Reactive and Functional Polymers* (2022) 181, 105419 <https://doi.org/10.1016/j.reactfunctpolym.2022.105419> (FI = 5.1), (Q1).

5. **B.-I. Ciubotaru**, M.-F. Zaltariov, C. Tugui, E. Stoleru, D. Peptanariu, G. Stiubianu, N. Vornicu, M. Cazacu, Silicones with different crosslinking patterns: Assessment from the perspective of their suitability for biomaterials, *Surfaces and Interfaces* (2022) 32, 102168, <https://doi.org/10.1016/j.surfin.2022.102168>. F.I. =6.2, (Q1).

Conferences:

1. I. Grădinaru, **B.-I. Ciubotaru**, M. Dascălu, Preliminary study concerning the adaptation of a periodontal dressing material to the inclusion of therapeutic agents, EUROINVENT ICIR 2023, International Conference on Innovative Research, Iasi, 11th–12st of May 2023

2. I. Grădinaru, A. Bargan, **B.-I. Ciubotaru**, Dynamic Vapour Sorption Analysis in the Preliminary Evaluation of Silicone Impression Materials, The 11th IEEE International Conference on E-Health and Bioengineering - EHB 2023, Grigore T. Popa University of Medicine and Pharmacy Iasi, November 9-10, 2023, Bucharest, Romania

3. I. Gradinaru, **B.-I. Ciubotaru**, M. Dascălu, A. Bargan, A.-L. Vasiliu, Alginate dental impression materials with Allantoin enrichment: a morphology, dynamic vapor sorption and swelling evaluation, IEEE E-HEALTH AND BIOENGINEERING CONFERENCE - EHB 10-th edition, Iași, Romania, November 17-19, 2022

4. M.-F. Zaltariov, A. Bargan, D. Peptanariu, C. Cojocaru, **B.-I. Ciubotaru**, M. Cazacu, Bioactive and biodegradable silatranes as potential functional entities for nanoplatfroms of biomedical relevance, Congresul Internațional al Universității Apollonia „Pregătim viitorul, promovând excelența”, Iași, România, 28 februarie - 2 martie 2022

5. **B.-I. Ciubotaru**, C. Țugui, M. Cazacu, N. Vornicu, M.-F. Zaltariov, Silicone materials-from cultural heritage conservation to biomedical applications, Conferința științifică internațională PATRIMONIUL CULTURAL DE IERI –IMPLICAȚII ÎN DEZVOLTAREA SOCIETĂȚII DURABILE DE MÂINE, CULTURAL HERITAGE OF YESTERDAY – CONTRIBUTION TO THE DEVELOPMENT OF A SUSTAINABLE SOCIETY OF TOMORROW, ediția a V-a, Iași-Chișinău, 22 Februarie 2022

6. Irina Gradinaru, Bianca-Iulia Ciubotaru and Ana-Lavinia Vasiliu, A Morphological and Structural Study of Four Elastomeric Impression Materials Used in Dental Medicine, IEEE E-HEALTH AND BIOENGINEERING CONFERENCE - EHB 2021, 9-th edition, Iași, Romania, November 18-19, 2021

7. **B.-I. Ciubotaru**, M. Cazacu, Evaluation of silicone-based biomaterials from the bio- and mucoadhesive perspective, MacroYouth, SESIUNEA DE COMUNICĂRI ȘTIINȚIFICE A TINERILOR CERCETĂTORI POARTĂ DESCHISĂ SPRE VIITOR, 19 Noiembrie 2020, Iași, România

8. B.-I. Ciubotaru, I. Gradinaru, M.-F. Zaltariov, M. Cazacu, Comparative study on the characteristics of silicone synthetic elastomers used in dental impression techniques; International Conference on Innovative Research - ICIR EUROINVENT 2020, Iasi, Romania, 21-22 Mai, 2020

9. B.-I. Ciubotaru, M.-F. Zaltariov, M. Cazacu, C. Racles, Functionalized mesoporous silica in drug delivery and biomedical applications; Congresul Internațional al Universitatii “Apollonia” Editia a XXX-a „Pregătim viitorul promovând excelența”, Iași, România, 27 februarie – 1 martie 2020

10. B.-I. Ciubotaru, M.-F. Zaltariov, C. Racles, M. Cazacu, Functionalized mesoporous silica as carrier for controlled delivery of doxorubicin; „ZILELE SPITALULUI CLINIC C.F. IASI” 2019 - PERFORMANTA Stiintei – STIINTA PERFORMANTEI, Iasi, Romania, 22-27 octombrie 2019

11. L. Verestiuc, B. I. Ciubotaru, Smart Mucoadhesive Polymeric Biomaterials for Medical /Pharmaceutical Applications and in Vitro Models for Their Evaluation. In: ICNMBE: International conference on Nanotechnologies and Biomedical Engineering: proc. of the 4rd intern. conf., Sept. 18-21 : Program & Abstract Book , 2019. Chișinău, 2019, p. 112. ISBN 978-9975-72-392-3

Posters:

1. B.-I. Ciubotaru, A. Bargan, G. Știubianu, M. Dascălu, A.-M. Macsim, A. Bele, A. Soroceanu, The development and characterization of new membranes based on polysulfone and silsesquioxanes with perspectives in environmental applications, 112th International Conference on Environmental Engineering and Management (ICEEM), 13-16 September 2023, Iași, Romania

2. B.-I. Ciubotaru, M. Dascălu, A. Bele, M.-F. Zaltariov, Functional silicone elastomers efficiently crosslinked through supramolecular interactions without catalyst, 10th European Silicon Days, Montpellier, France, 10-12 July 2023

3. G. Stiubianu, B.-I. Ciubotaru, M. Dascalu, A. Bele, V. Tiron, Solvent-free silicone-based elastomers with self-healing capabilities by supramolecular interactions, Annual Polymer Day, Lyngby, Denmark, 30 Septembrie 2022

4. A. Bele, M. Dascalu, G. Stiubianu, B.-I. Ciubotaru, V. Carlescu, V. Tiron, I. Burducea, A. Pandeale, Silicone-based modular artificial sensing skin for MMOD impact damage detection and evaluation system in spacecraft, International Exhibition of Inventions INVENTICA, Iași, România, 22 – 24.06.2022

5. B.-I. Ciubotaru, M.-F. Zaltariov, C. Racles, M. Cazacu, Preparation and application of mesoporous silica for pH-controlled delivery of doxorubicin, Zilele Universității „Alexandru Ioan Cuza” din Iași Conferința FACULTĂȚII DE CHIMIE IasiChem 2019, 31 Octombrie – 01 Noiembrie, 2019

ISI articles related to the thesis field:

1. Gradinaru, I., **Ciubotaru, B.-I.**, Butnaru, M., Cojocaru, F.D., Covașă, C.T., Bibire, T., Dascalu, M., Bargan, A., Cazacu, M. and Zaltariov, M.F., 2023. The Impact of the Addition of Vitamins on a Silicone Lining Material to the Oral Mucosa Tissue—Evaluation of the Biocompatibility, Hydrolytic Stability and Histopathological Effect. *Medicina*, 59(11), p.1936.
2. Gradinaru, I., Vasiliu, A.L., Bargan, A., Checherita, L.E., **Ciubotaru, B.I.**, Armencia, A.O., Istrate, B., Dascalu, C.G. and Antohe, M.E., 2023. The Influence of Beverages on Resin Composites: An In Vitro Study. *Biomedicines*, 11(9), p.2571.
3. I. Gradinaru, A. L. Vasiliu, A. Bargan, **B.-I. Ciubotaru**, A. O. Armencia, L. L. Hurjui, L. E. Checheriță, C. G. Dascalu, M.-E. Antohe, Evaluation of the behaviour of dental composites related to different types of drinks by the dynamic vapor sorption method, Romanian Journal of Oral Rehabilitation, Vol. 15, no. 2, pp. 328 – 335, 2601-4661.
4. I. Grădinaru, **B-I Ciubotaru**, M. Dascălu, Preliminary study concerning the adaptation of a periodontal dressing material to the inclusion of therapeutic agents, Archives of Metallurgy and Materials, accepted for publication
5. D. Filip, D. Macocinschi, M.-F Zaltariov, **B.-I. Ciubotaru**, A. Bargan, C.-D. Varganici, A.-L. Vasiliu, D. Peptanariu, M. Balan-Porcarasu, M.-M. Timofte-Zorila, Hydroxypropyl Cellulose/Pluronic-Based Composite Hydrogels as Biodegradable Mucoadhesive Scaffolds for Tissue Engineering, Gels., 8, 519 (2022), <https://doi.org/10.3390/gels8080519>
6. G.-T. Stiubianu, A. Bele, M. Grigoras, C. Tugui, **B.-I. Ciubotaru**, M.-F. Zaltariov, F. Borza, L.-G. Bujoreanu, M. Cazacu, Scalable Silicone Composites for Thermal Management in Flexible Stretchable Electronics, Batteries., 8(8), 95 (2022), <https://doi.org/10.3390/batteries8080095>
7. **B.-I. Ciubotaru**, M.-F. Zaltariov, C. Tugui, E. Stoleru, D. Peptanariu, G. Stiubianu, N. Vornicu, M. Cazacu, Silicones with different crosslinking patterns: Assessment from the perspective of their suitability for biomaterials, Surf. Interfaces., 32, 102168 (2022), <https://doi.org/10.1016/j.surfin.2022.102168>
8. D. Filip, D. Macocinschi, M.-F. Zaltariov, C.A. Gafitanu, C.G. Tuchilus, A. Bele, **B.-I. Ciubotaru**, E. Stoleru, A. Bargan, Mucoadhesive and Antimicrobial Allantoin/ β Cyclodextrins-Loaded Carbopol Gels as Scaffolds for Regenerative Medicine, Gels, 8(7), 416 (2022), <https://doi.org/10.3390/gels8070416>
9. C. Racles, M. Asandulesa, V. Tiron, C. Tugui, N. Vornicu, **B.-I. Ciubotaru**, M. Miřcuřsik, M. Omastov´a, A. L. Vasiliu, C. Ciomaga, Elastic Composites with PDMS matrix and Polysulfone-Supported Silver Nanoparticles as Filler, Polymer 217 (2021) 123480, <https://doi.org/10.1016/j.polymer.2021.123480>

10. Spiridon, I.; Andrei, I.-M.; Anghel, N.; Dinu, M.V.; **Ciubotaru, B.-I.** Development and Characterization of Novel Cellulose Composites Obtained in 1-Ethyl-3-methylimidazolium Chloride Used as Drug Delivery Systems. *Polymers* 2021, 13, 2176. <https://doi.org/10.3390/polym13132176>

11. Spiridon, I.; Anghel, N.; Dinu, M.V.; Vlad, S.; Bele, A.; **Ciubotaru, B.I.**; Verestiuc, L.; Pamfil, D. Development and Performance of Bioactive Compounds-Loaded Cellulose/Collagen/Polyurethane Materials, *Polymers* 2020, 12, 1191. <https://doi.org/10.3390/polym12051191>

12. D. Macocinschi, D. Filip, **B.-I. Ciubotaru**, R.P. Dumitriu, C.-D. Varganici, M.-F. Zaltariov, Blends of sodium deoxycholate-based poly(ester ether)urethane ionomer and hydroxypropylcellulose with mucosal adhesiveness, *International Journal of Biological Macromolecules* 162 (2020) 1262–1275, <https://doi.org/10.1016/j.ijbiomac.2020.06.191>

13. I. Grădinaru, **B.-I. Ciubotaru**, M.F. Zaltariov, An Attenuated Total Reflectance study of different alginate impression materials used in dental medicine, *The Medical-Surgical Journal*, 2020, 4 (124).

14. M.-F. Zaltariov, **B.-I. Ciubotaru**, L. Vereștiuc, D. Peptanariu, D. Macocinschi, D. Filip, Ruthenium (II) complexes with cytotoxic activity embedded in hydroxypropyl methylcellulose/sodium alginate mucoadhesive hydrogels, *CELLULOSE CHEMISTRY AND TECHNOLOGY*, Volume 53, Issue 9-10 September-December, p. 869-878

15. N. Anghel, S. Lazăr, **B.-I. Ciubotaru**, L. Vereștiuc, I. Spiridon, New cellulose-based materials as transdermal transfer systems for bioactive substances, *CELLULOSE CHEMISTRY AND TECHNOLOGY*, Volume 53, Issue 9-10 September-December, p.879-884

16. I Grădinaru, **B-I Ciubotaru**, M-F Zaltariov and M Cazacu, Comparative Study on the Characteristics of Silicone Elastomers used inDental Impression TechniquesIOP Conference Series Materials Science and Engineering, July 2020, DOI: 10.1088/1757-899X/877/1/012036

Book chapters:

1. M.-F. Zaltariov, **B.-I. Ciubotaru**, M. Savin, D. Filip, D. Macocinschi, Bio-Based Polymers For Liposomal Drug Formulations In book: Applications of Biodegradable and Bio-Based Polymers for Human Health and a Cleaner Environment, Nov 2021, Apple Academic Press, partnered with CRC Press, a member of the Taylor & Francis Group, ISBN: 9781771889766, DOI: 10.1201/9781003146360-5

Additional courses in related fields:

Bianca-Iulia Ciubotaru, e-SPACE Heart Failure 2023, EBAC Cert-ID: 2023-EPN-9741000-000, 10 CME credits, Course Director Prof. Stefan D. Anker, October 20-21, 2023

Ciubotaru Bianca-Iulia, Proiectarea activităților de cercetare în studii europene: documentare, metode și diseminare (C5), Jean Monnet Module on EU Interdisciplinary Studies: Widening Knowledge for a more Resilient Union EURES-621262-EPP-1-2020-1-RO-EPPJMO, Course Director- Cercet. (II) dr. Ramona Țigănașu, Iași, July 2021

Traineeships and mobilities:

Taras Shevchenko National University of Kyiv, Ucraina, 28.08.2021-27.10.2021, H2020-MSCA-RISE-2016 project, SPINSWITCH No 734322

Projects:

1. Mimicking living matter mechanisms by five-dimensional chemistry- 5D-nanoP, Project code: PN-III-P4-ID-PCCF-2016-0050, Contract no. 4/2018, team member between 2019-2022

2. Emerging 2D materials based on two-dimensional permethylated metal-organic networks- 2D-PerMONSil, PN-III-P4-ID-PCE-2020-2000, PCE 207/2021, team member between 2021-2023

3. Silicone-based modular artificial sensing skin for MMOD impact damage detection and evaluation system in spacecraft Force sensors with self-healing properties – SilArtSkin, PN-III-P1-1.1-TE-2021-0156, team member 2022-present